8.9 Global Warming Potential

The *Global Warming Potential* (GWP) is a weighting factor that allows comparisons to be made between the cumulative global warming impact over a specified period of time of some greenhouse gas and a simultaneous emission of an equal mass of CO_2. There are three primary factors that affect GWPs. The first is the radiative forcing associated with the addition to the atmosphere of a unit mass of each greenhouse gas. The second is based on estimates of the rate at which that unit mass injected decays over time. The third is related to the cumulative radiative forcing that the unit addition to the atmosphere will have over some period of time into the future.

Some examples of how the GWP index can be used include the following:

1. By combining GWP with estimates of the cost of curtailing emissions of each greenhouse gas, a country-by-country, least-cost approach to prevention of climate change could be identified.
2. GWPs could facilitate trading of emissions reductions among countries. For example, one country might decide the least expensive way to offset emissions of CO_2 might be to reduce emissions of CH_4 in another. Buying and selling international carbon emission offsets could lead to technology and economic transfer from the developed to the developing countries (Swisher and Masters, 1991).
3. Country by country rankings of their individual contributions to climate change are made possible. Quantifiable goals can then be established for future reductions.
4. Combined with other indices, they could be part of an overall environmental impact assessment for products and industrial process audits. Included in an environmental labeling system, consumer choices could be affected.

Calculating the GWP

Mathematically, we imagine an impulse function in which 1 kg of the greenhouse gas in question and 1 kg of CO_2 are emitted into the atmosphere at the same time. As the concentration of each gas decreases with time, so does the radiative forcing associated with the remaining amount of gas. Mathematically, the GWP of a greenhouse gas is given by

$$\mathrm{GWP}_g = \frac{\displaystyle\int_0^T F_g \cdot R_g(t)\, dt}{\displaystyle\int_0^T F_{CO_2} \cdot R_{CO_2}(t)\, dt} \tag{8.43}$$

where

F_g = radiative forcing efficiency of the gas in question, $(W/m^2)/kg$
F_{CO_2} = radiative forcing efficiency of CO_2, $(W/m^2)/kg$
$R_g(t)$ = fraction of the 1 kg of gas remaining in the atmosphere at time t
R_{CO_2} = fraction of the 1 kg of CO_2 remaining at time t
T = the time period for cumulative effects (years)

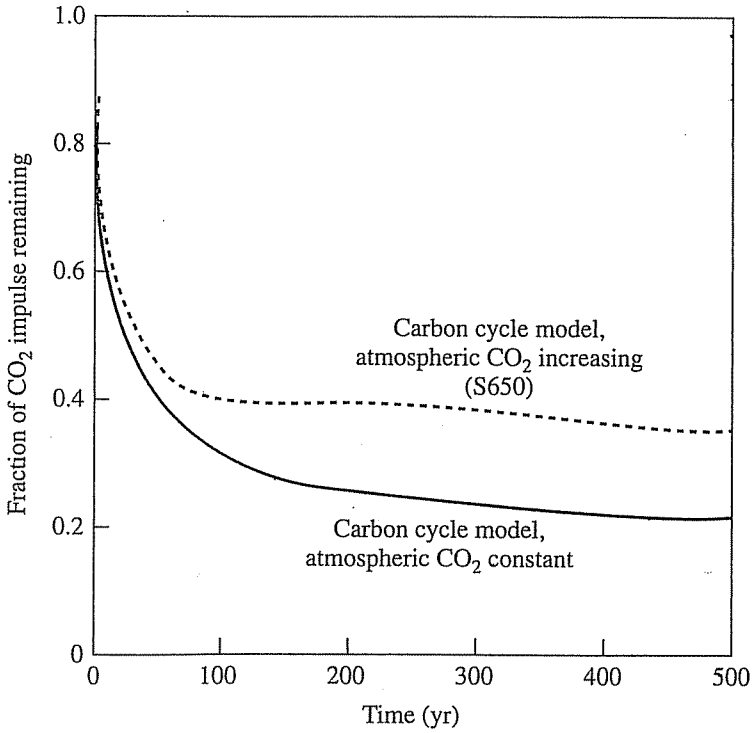

FIGURE 8.30 The impulse response for an injection of 1 kg of CO_2 into the atmosphere; that is, $R_{CO_2}(t)$ in (8.43). The solid line is for an atmosphere in which the CO_2 concentration is constant; the dashed line is for an atmosphere that stabilizes at 650 ppm of CO_2 by the year 2200. (*Source:* IPCC, 1995.)

For some greenhouse gases, R_g can be modeled using a simple exponential decay function. And for some, the radiative efficiency is a constant. Neither is the case for the comparison gas, CO_2. As Figure 8.30 suggests, CO_2 decay is rapid during the first few decades as the biosphere absorbs the carbon, and then for next few hundred years, it decays at a much slower rate corresponding to the slow uptake of the oceans. To further complicate matters, the decay also depends on the assumptions made for the background concentration of CO_2. Two curves for R_{CO_2} are shown, one corresponding to an atmosphere in which CO_2 concentration is unchanging, while the other has been drawn for a more realistic atmosphere in which CO_2 reaches 650 ppm by the year 2200.

The choice of the GWP time horizon that policy makers might use depends on the issues that are being addressed. For example, shorter time horizons might be used when it is the rate of change of global temperature, rather than the ultimate temperature increase, that is of concern. Short time horizons would also seem appropriate when the most effective greenhouse abatement strategy is needed to head off possibly abrupt climate changes that might be triggered when warming reaches some threshold level. On the other hand, long time horizons might be used to evaluate strategies to avoid long, slow, irreversible impacts such as sea level changes.

Carbon Dioxide Equivalents of Greenhouse Gases

Table 8.7 shows GWPs for a number of widely used chemicals. As can be seen, all of these species have very high GWPs relative to CO_2 because they all absorb in the atmospheric window. Notice the three standard time horizons for GWPs are 20 years, 100 years, and 500 years. By including a time horizon, the GWP accounts for the

TABLE 8.7

Global Warming Potentials (GWPs) Relative to Carbon Dioxide (kilograms of CO_2 per kilogram of gas)

Chemical Species	Chemical Formula	Lifetime (yrs)	Global Warming Potential (Time Horizon in Years) 20-yr	100-yr	500-yr
Carbon dioxide	CO_2	50–200	1	1	1
Methane	CH_4	12	62	23	7
Nitrous oxide	N_2O	114	275	296	156
CFC-11	$CFCl_3$	45	6,300	4,600	1,600
CFC-12	CF_2Cl_2	100	10,200	10,600	5,200
CFC-113	$CF_2ClCFCl_2$	85	6,100	6,000	2,700
CFC-115	CF_3CClF_2	1,700	4,900	7,200	9,900
HCFC-22	CHF_2Cl	12	4,800	1,700	540
HCFC-141b	CH_3CFCl_2	9.3	2,100	700	220
HCFC-142b	CH_3CF_2Cl	19	5,200	2,400	740
HFC-23	CHF_3	270	9,400	11,700	10,000
HFC-134a	CH_2FCF_3	14	3,300	1,300	400
HFC-152a	CH_3CHF_2	1.4	410	120	37
Tetrafluoromethane	CF_4	50,000	3,900	5,700	8,900
Hexafluoroethane	C_2F_6	10,000	8,000	11,900	18,000
Sulfur hexafluoride	SF_6	3,200	15,100	22,200	32,400
Carbon tetrachloride	CCl_4	35	2,700	1,800	580
Methyl bromide	CH_3Br	1	16	5	1
Halon-1301	CF_3Br	65	7,900	6,900	2,700

Source: IPCC, 3rd Assessment, 2001.

greater impact that a gas with a long atmospheric lifetime will have compared with one that quickly disappears after it has been emitted. For example, CFC-115 and a replacement HCFC-22 have almost identical 20-year GWPs, but the longer atmospheric lifetime of CFC-115 (1,700 vs. 12 years) means its 100-year GWP is more than five times higher (7,200 vs. 1,700), and its 500-year GWP is almost 20 times higher.

Notice the extremely high GWPs for several gases in this table. Some of the HFCs, which were developed as alternatives to ozone-depleting substances, stand out—especially trifluoromethane (HFC-23). HFC-23 has a lifetime of 270 years and a 100-yr GWP of 11,700. Reducing HFC-23 in developing countries has become one of the most sought-after (least expensive) approaches to meeting Kyoto Protocol obligations. The perfluorocarbons CF_4 (tetrafluoromethane) and C_2F_6 (hexafluoroethane), used in semiconductor manufacturing and primary aluminum production, have extremely long atmospheric lifetimes and GWPs thousands of times higher than CO_2. One gas, sulfur hexafluoride (SF_6) has a GWP of 22,200, which gives it the distinction of being the most potent greenhouse gas the IPCC has ever evaluated. SF_6 has excellent dielectric properties and was widely used in electric power and distribution equipment.

The purpose of the GWPs is to assess the relative importance of various emissions, which means the GWP for each gas should be multiplied by the emission rate for the gas. The 100-year GWPs are often used to describe non-CO_2 emissions in terms of *carbon dioxide equivalents* (CDE, or CO_2-eq), as Example 8.11 demonstrates.

EXAMPLE 8.11 Carbon Dioxide Equivalent of Greenhouse Gases

Annual anthropogenic emissions of CO_2, CH_4, and N_2O are estimated to be 27,000 $MtCO_2$/yr, 370 $MtCH_4$/yr, and 6 MtN_2O/yr (where "Mt" means million metric tons). Compare the impacts of these three gases over a 100-year time horizon, and find the total equivalent CO_2 emissions.

Solution The comparison will be based on the products of emission rates and GWPs. GWPs are found in Table 8.7, and the emission rates are given. Carbon dioxide has a GWP of 1 (by definition) over all of the time horizons, so its product doesn't change:

CO_2: $GWP_{100} \times \text{emissions} = 1 \times 27{,}000 \text{ Mt/yr} = 27{,}000 \text{ MtCO}_2$

CH_4: $GWP_{100} \times \text{emissions} = 23 \times 370 \text{ Mt/yr} = 8{,}510 \text{ MtCO}_2\text{-eq}$

N_2O: $GWP_{100} \times \text{emissions} = 296 \times 6 \text{ MtN}_2\text{O/yr} = 1{,}776 \text{ MtCO}_2\text{-eq}$

The total carbon dioxide equivalence of the combined emissions is

$$27{,}000 + 8{,}510 + 1{,}776 = 37{,}286 \text{ MtCO}_2\text{-eq}$$

If we multiply this by the C/CO_2 ratio of 12/44 and switch the units, we can get an equivalence expressed in gigatons of carbon:

$$\text{Total } CO_2, CH_4, N_2O \text{ emissions} = 37.3 \text{ GtCO}_2\text{-eq} \times 12/44 = 10.1 \text{ GtC-eq}$$

Of this 10.1 GtC total, 7.4 GtC is actual carbon dioxide, and 2.8 GtC is other gases.

Example 8.11 suggests that almost three-fourths of the impact for the next century from current emissions of the three key greenhouse gases will be caused by CO_2. If we redo the calculations using 20-year GWPs, the near-term importance of controlling methane emissions stands out. Over the next 20 years, today's CH_4 emissions will have nearly as much impact on climate (85 percent as much) as today's CO_2 emissions.

Applying the above carbon dioxide equivalence approach to emissions puts the combination of greenhouse gases into perspective. Figure 8.31 shows the GWP-weighted emissions of U.S. greenhouse gases, and Figure 8.32 shows a "spaghetti chart" representation of their sources and the end uses responsible for those emissions.

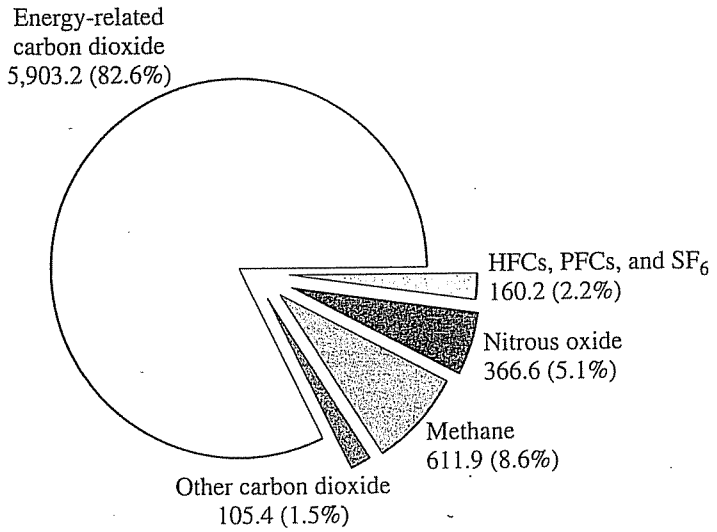

FIGURE 8.31 U.S. greenhouse gas emissions using 100-year GWPs (millions of metric tons of CO_2 equivalents and percentages of the total. (*Source:* EIA, 2006.)

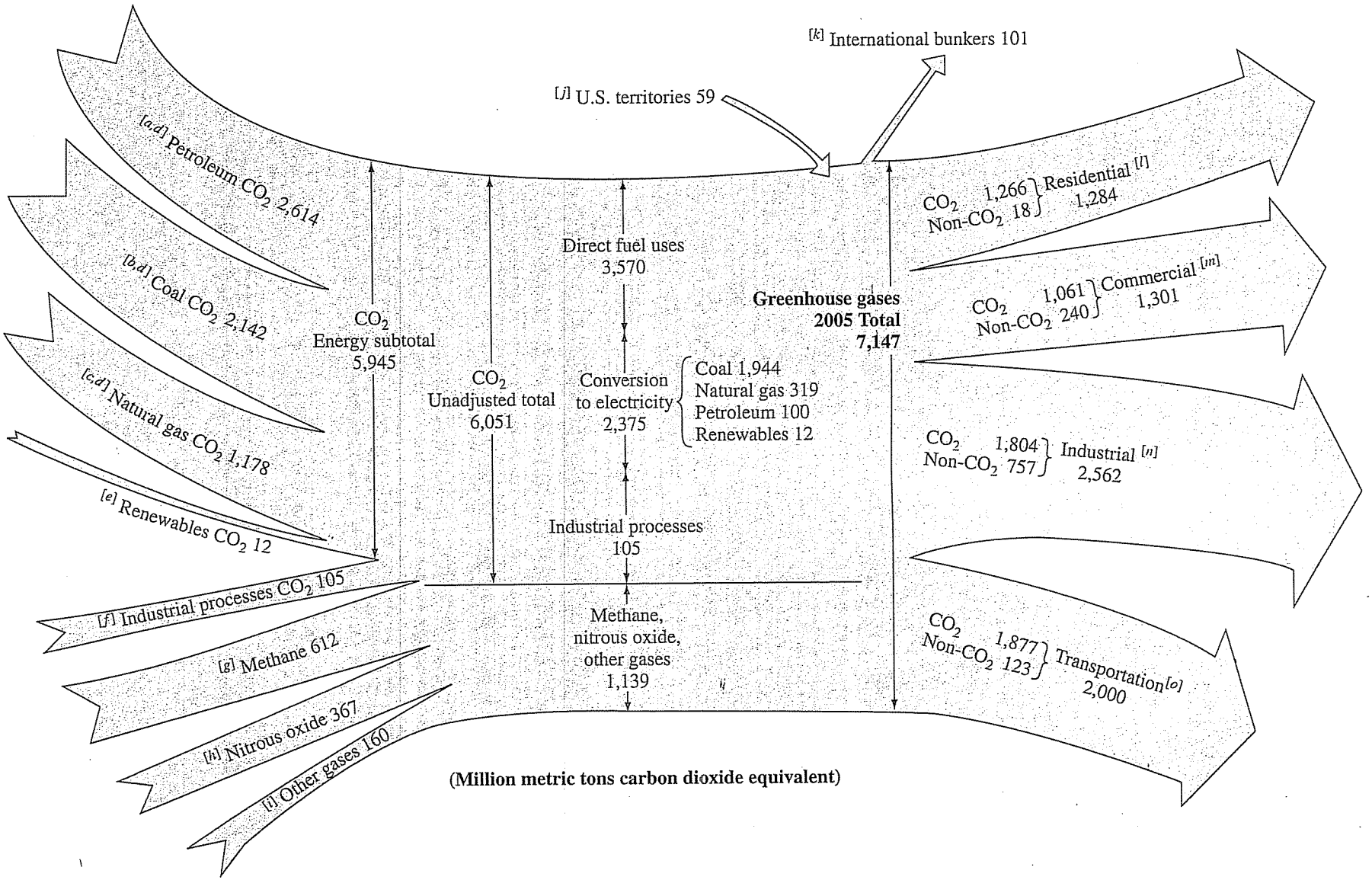

FIGURE 8.32 Greenhouse gas emissions in the U.S. economy, 2005.
(*Source:* EIA, 2006.)

EXAMPLE 8.12 Water Heater Emissions, Including Leakage

In Example 8.6, CO_2 emissions from a coal-fired power plant delivering power to an electric water heater were compared with emissions for a natural-gas-fired water heater.

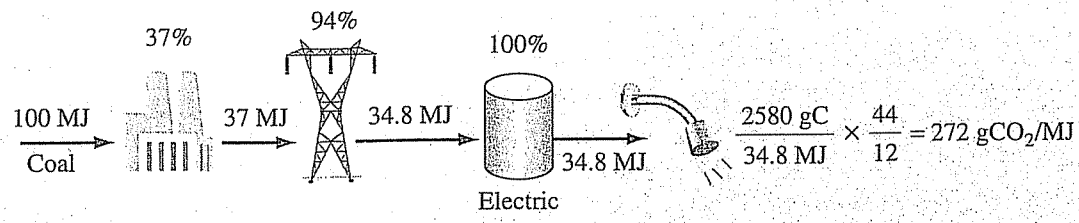

That analysis, however, didn't include the global warming impacts of the roughly 1.5 percent methane leakage to the atmosphere during the mining, transportation, and storage of natural gas before the gas makes it to the house. Including that leakage, what is the equivalent carbon emission rate for the 85 percent-efficient gas water heater? Use the 20-year GWP for natural gas.

Solution Starting with 100 MJ of natural gas, we'll lose 1.5 MJ in leakage and deliver 98.5 MJ to the gas-fired water heater.

From Table 8.3, the LHV carbon intensity of natural gas is 15.3 gC/MJ. From Table 8.7, the 20-year GWP of methane is 62 gCO_2/gCH_4. So, the CO_2 equivalent of that 1.5 MJ of methane leakage is

$$1.5\ \text{MJ} \times 15.3\ \text{gC/MJ} \times \frac{16\ \text{gCH}_4}{12\ \text{gC}} \times \frac{62\ \text{gCO}_2}{\text{g CH}_4} = 1{,}897\ \text{gCO}_2\text{-eq}$$

The actual CO_2 emissions from the 85 percent-efficient water heater are

$$\text{CO}_2\ \text{emissions} = 15.3\ \text{gC/MJ} \times 98.5\ \text{MJ} \times \frac{44\ \text{gCO}_2}{12\ \text{gC}} = 5{,}525\ \text{gCO}_2$$

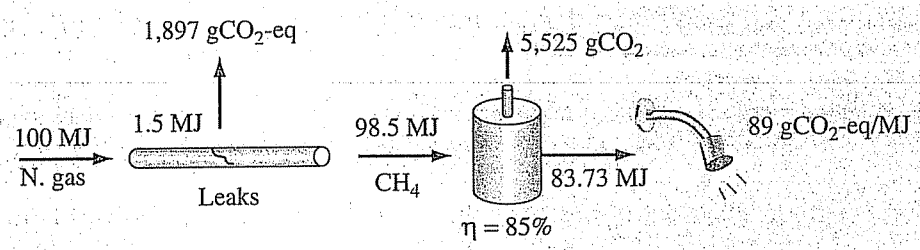

Total emissions from the gas-fired water heater per MJ actually heating water are

$$\frac{1{,}897\ \text{gCO}_2\text{-eq} + 5{,}525\ \text{gCO}_2}{83.73\ \text{MJ heat to water}} = 89\ \text{gCO}_2\text{-eq/MJ}$$

which is still a 68 percent savings compared to the 272 gCO_2 for the electric water heater (without including the leakage, the savings in Example 8.6 was 75 percent).

8.10 IPCC Assessment Reports

The Intergovernmental Panel on Climate Change (IPCC) is an organization founded in 1988 by the United Nations Environment Program (UNEP) and the World Meteorological Organization (WMO). Its role is to assess scientific, technical, and socioeconomic information related to the risks, potential impacts, and options for adaptation and mitigation of human-induced climate change. The IPCC itself does not carry out research but instead relies on literally thousands of climate and policy experts from around the globe who contribute their expertise as authors and reviewers of IPCC reports. Its principal output has been a series of assessment reports, which are based on peer-reviewed and published scientific and technical literature. The first IPCC Assessment Report, completed in 1990, provided the overall scientific and policy basis for addressing climate change adopted by the 1992 UN Framework Convention on Climate Change (UNFCCC), which entered into force in 1994. The Second Assessment Report (SAR), *Climate Change 1995,* was instrumental in negotiations that led to the adoption of the Kyoto Protocol by the UNFCCC in 1997.

The Third Assessment Report (TAR), *Climate Change 2001,* and the Fourth Assessment Report (AR4), which was released in 2007, continue to be the most authoritative summary documents on the status of climate research. The IPCC also prepares special reports and technical papers to fill the gaps between those major, comprehensive assessment reports.

The IPCC is organized around three focus areas: Science (Working Group I), Impacts and Adaptation (Working Group II), and Mitigation (Working Group III). The mitigation group develops scenarios that describe possible combinations of population, economic growth, and technology drivers that lead to future greenhouse gas emissions. These emissions scenarios are then handed off to the climate modeling community, which converts them into regional and global temperatures and climate impacts. Those, in turn, can inform decision makers about the potential to mitigate these impacts (by modifying the emissions driving forces) and/or adapting to those climate changes (e.g., raise the levees). Figure 8.33 summarizes these interactions and helps frame the climate problem in terms of both sustainable development and environment.

The Special Report on Emissions Scenarios (SRES)

The IPCC *Special Report on Emissions Scenarios* (SRES) published in 2000 is based on a set of four storylines that weave demographic, technological, and economic driving forces into four distinct scenarios that can be translated into future emissions. Scenarios provide alternative images about how the future might unfold. They are not forecasts, nor do they carry with them any probabilities of their likelihood. No preferences for one scenario over another are offered by IPCC, and they are not meant to infer policy recommendations. They are narratives, around which emission scenarios can be built.

The SRES report describes four narrative storylines, designated as A1, A2, B1, and B2. The A storylines focus more on economic growth, while the B storylines have more of an environmental emphasis. The A1 and B1 lines are based on more of a homogeneous, globalized future, while the A2 and B2 imagine a more fractured

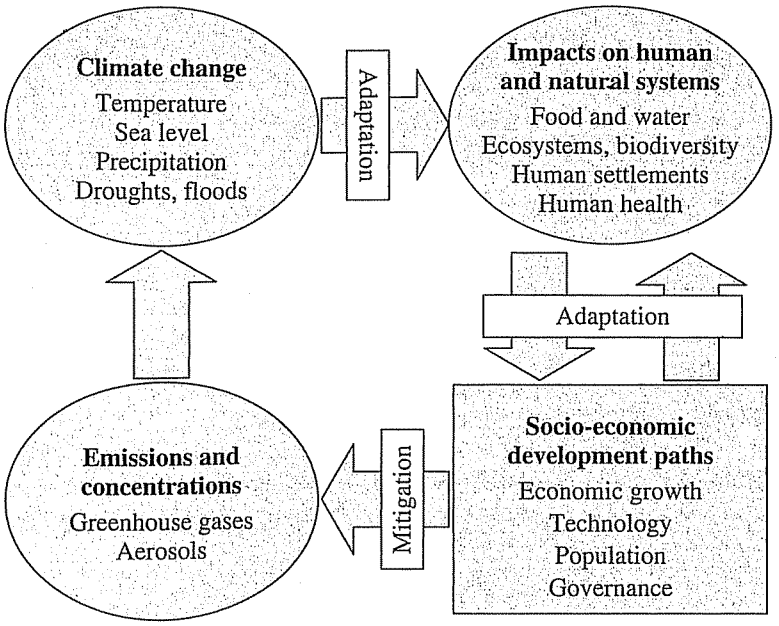

FIGURE 8.33 Sustainable development, adaptation, and mitigation interactions. (*Source:* IPCC, TAR, 2006.)

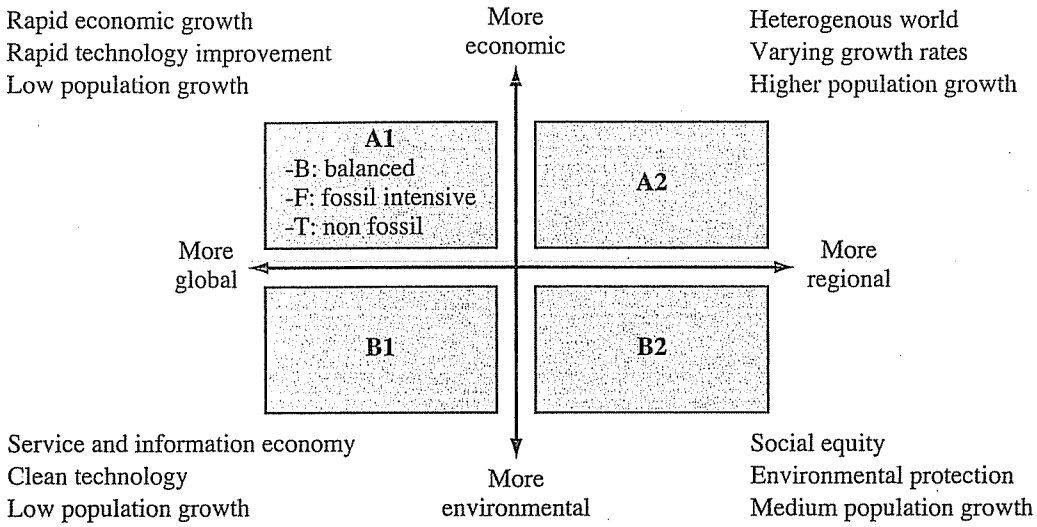

FIGURE 8.34 The four families of storylines in the SRES emission scenarios.

world with different regional priorities and growth rates. The A1 line is further designated to be either fossil-fuel intensive (A1-F), nonfossil fuel, technology emphasis (A1-T), or a more balanced combination of the two (A1-B). These characterizations are summarized in Figure 8.34.

Within each of the four storylines, multiple scenarios have been developed. Table 8.8 summarizes population, world GDP, and primary energy that result from a single illustrative scenario for each of the six categories (A1F, A1B, A1T, A2, B1, B2), but in reality there are many more within each category. One clue to the emphasis placed on technology in each scenario is the relative dependence on coal versus zero-carbon energy sources for each scenario, also shown in the table. Carbon dioxide emissions that result from these scenarios are shown in Figure 8.35.

TABLE 8.8

Some Main Driving Forces for Illustrative Scenarios from the Six SRES Storylines (each of the six categories has multiple scenarios not shown)

	A1F1	A1B	A1T	A2	B1	B2
Population (billion)						
1990	5.3	5.3	5.3	5.3	5.3	5.3
2020	7.6	7.5	7.6	8.2	7.6	7.6
2050	8.7	8.7	8.7	11.3	8.7	9.3
2100	7.1	7.1	7.0	15.1	7.9	10.4
World GDP (10^{12} $1990/yr)						
1990	21	21	21	21	21	21
2020	53	56	57	41	53	51
2050	164	181	187	82	136	110
2100	525	529	550	243	328	235
Primary Energy (10^{18}J/yr)						
1990	351	351	351	351	351	351
2020	669	711	649	595	606	566
2050	1431	1347	1213	971	813	869
2100	2073	2226	2021	1717	514	1357
Share of Coal in Primary Energy (%)						
1990	24	24	24	24	24	24
2020	29	23	23	22	22	17
2050	33	14	10	30	21	10
2100	29	4	1	53	8	22
Share of Zero Carbon in Primary Energy (%)						
1990	18	18	18	18	18	18
2020	15	16	21	8	21	18
2050	19	36	43	18	30	30
2100	31	65	85	28	52	49

Source: IPPC, SRES, 2000.

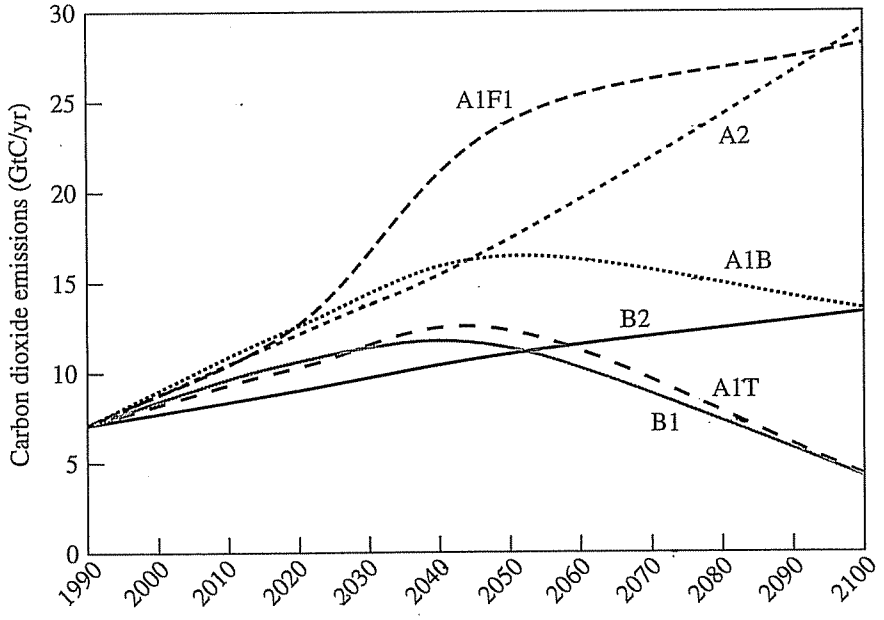

FIGURE 8.35 Illustrative SRES scenarios for fossil-fuel plus land-use carbon dioxide emissions corresponding to the scenarios shown in Table 8.8. (*Source:* Based on IPCC, SRES, 2000.)

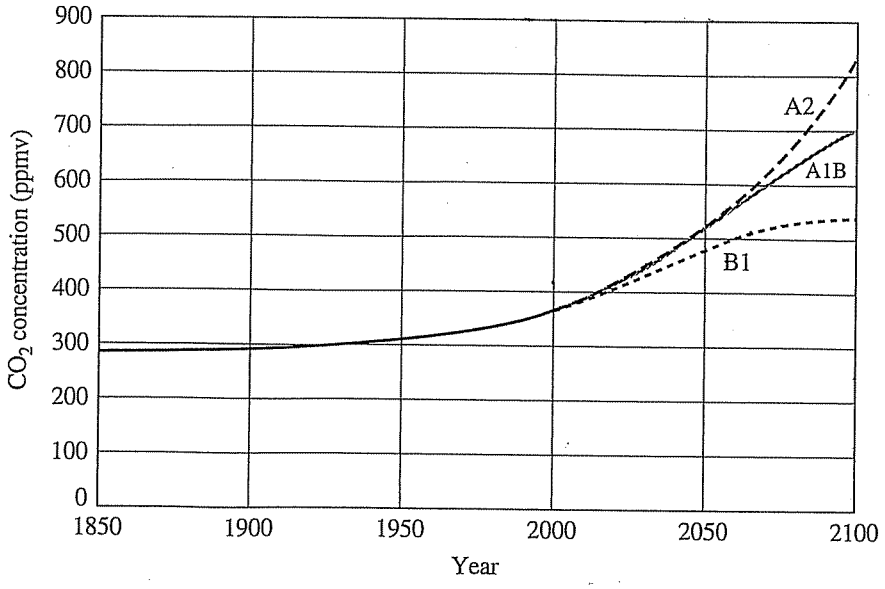

FIGURE 8.36 Simulations of CO_2 concentrations for three SRES scenarios done for the Fourth Assessment Report (AR4).
(*Source:* Max Planck Institute for Meteorology, 2006.)

The SRES scenarios provide estimates for greenhouse gas emissions over the next 100 years or so. Those emission rates can then be used as inputs for climate models that estimate future atmospheric concentrations of CO_2, CH_4, N_2O, and other greenhouse gases, from which GWP-weighted equivalent CO_2 concentrations can be estimated. Figure 8.36 shows one set of simulations done at the Max Planck Institute for Meteorology (MPI-M) in Hamburg for three of the SRES scenarios, A1B, A2, and B1, which cover the range of scenarios shown in Figure 8.35. Under the most optimistic scenario B1, CO_2 stabilizes at close to double the preindustrial concentration.

General Circulation Models

Scenarios for future greenhouse gas emissions are used as inputs to computer models that attempt to predict likely impacts of these perturbations on the Earth's climate systems. At this point in time, even the largest supercomputer cannot handle all of the mathematical complexity that could be included if scientists tried to model everything they know about how the climate system works. So, a hierarchy of models has been created, with the most sophisticated of those being *general circulation models* (GCMs). There are both atmospheric-GCMs and ocean-GCMs, which can be coupled together to form an atmospheric-ocean coupled general circulation model (AOGCM). As GCMs have evolved in complexity, they have gotten better and better at matching the historical record, which adds confidence in their predictions for the future. A complete global climate model would couple an AOGCM with a land model, a sea-ice model, and models for aerosols, carbon cycle, vegetation dynamics, and atmospheric chemistry.

A 3D (actually 4D if you include time) atmospheric general circulation model is based on a cartesian grid in which the atmosphere is divided into cells, such as are shown in Figure 8.37. For the ECHAM5/MPI-OM coupled atmosphere-ocean

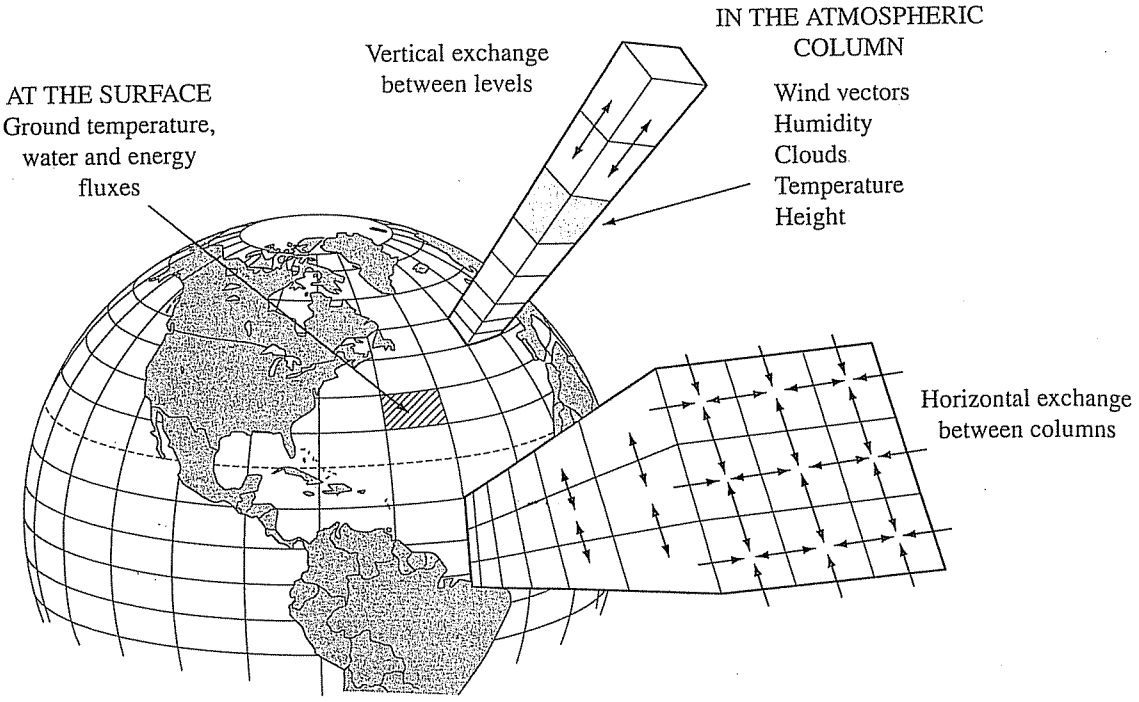

FIGURE 8.37 A cartesian (or rectangular) grid GCM in which horizontal and vertical exchanges are handled between adjacent columns and layers.
(*Source:* Based on Henderson-Sellers and McGuffie, 1987.)

model used at the Max Planck Institute for Meteorology in Germany, the cells have a horizontal resolution of approximately 200 km with 31 vertical levels. Their ocean GCM has regionally varying horizontal resolution between approximately 10 km and 150 km. Each cell is characterized by a number of variables such as temperature, humidity, pressure, cloudiness, and so forth. Those cells then communicate (mathematically) with adjacent atmospheric cells and are updated with some specified time increment. A grid coupling of atmosphere, ocean, and land models is shown in Figure 8.38.

Global Mean Temperature Simulations

After having run simulations for accumulating concentrations of carbon dioxide and other greenhouse gases, GCMS attempt to predict future global climate responses. A major uncertainty introduced at this stage of modeling is properly estimating the appropriate climate sensitivity factor, ΔT_{2X} (the change in mean global temperature resulting from a doubling of the equivalent CO_2 concentration above its preindustrial level).

The IPCC has often used three possible values of climate sensitivity, 1.5°C, 2.5°C, and 4.5°C, but a more recent approach has been based on trying to use a probability density function (pdf) and its accompanying cumulative probability distribution to help quantify the uncertainty in this key parameter. Figure 8.39 shows two such probability estimates. One (labeled WR, after its author's initials), is based on a log-normal fit to the long-stated IPCC 90 percent probability range for ΔT_{2X} of 1.5°C to 4.5°C. The WR pdf has a median ΔT_{2X} probability of 2.6°C and indicates a 10 percent chance that it is greater than 4°C. The other (labeled AS) has a median

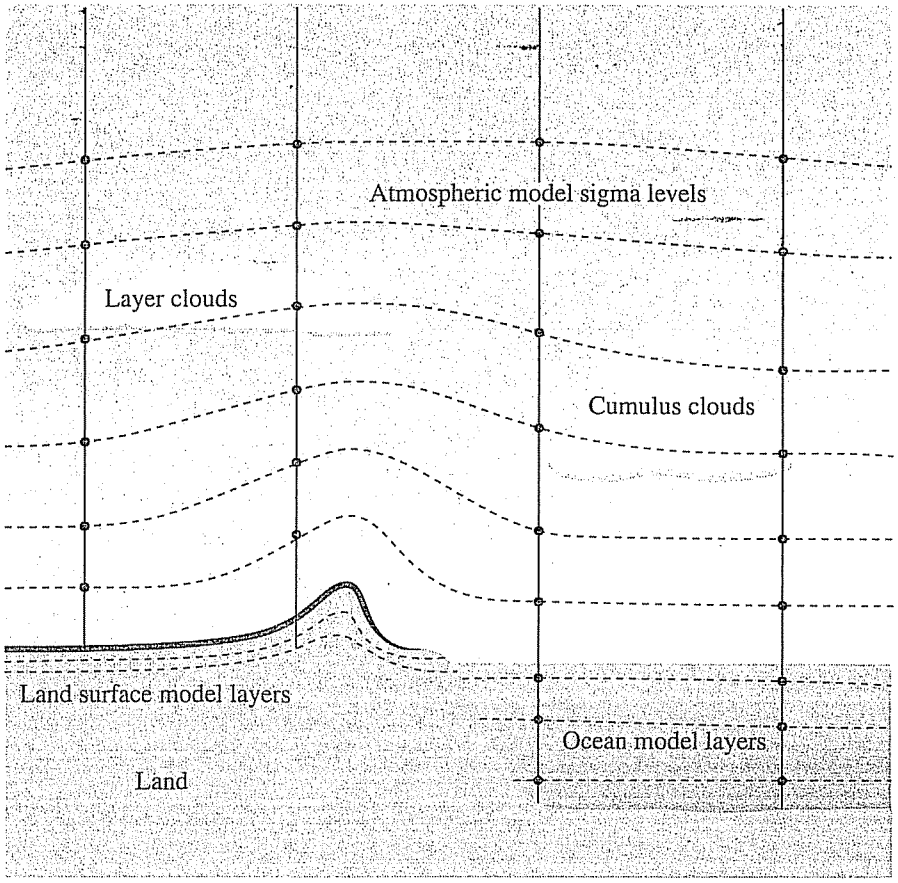

FIGURE 8.38 Coupled atmosphere, ocean, and land GCM grid.
(*Source:* Bureau of Meteorology, Australia.)

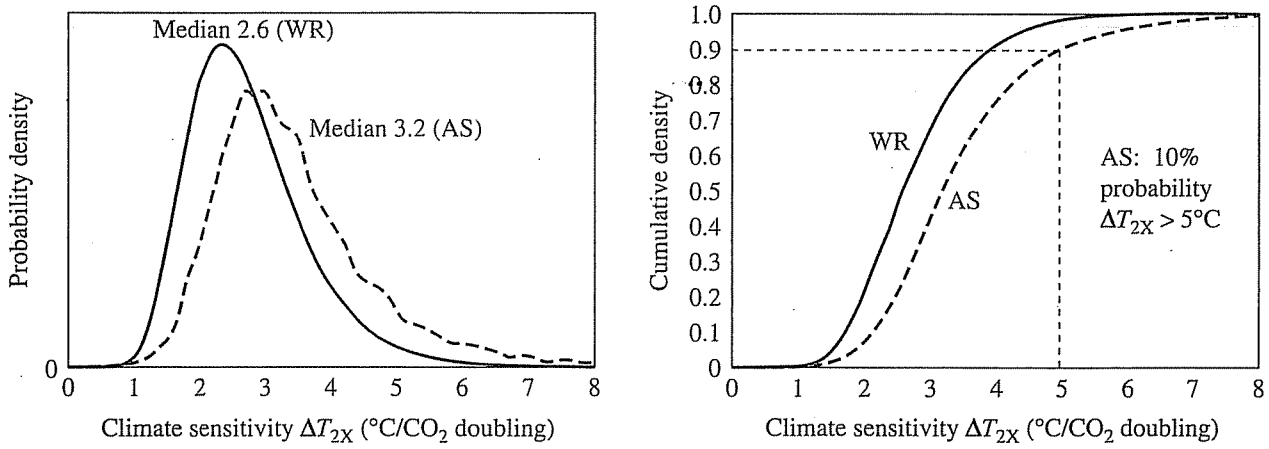

FIGURE 8.39 The probability density function and cumulative probability function for two estimates of the climate sensitivity factor, ΔT_{2X}. The dotted lines for the AS pdf indicate a 10 percent probability that the sensitivity factor is over 5°C.
(*Source:* WR = Wigley and Raper, 2001; AS = Andronova and Schlesinger, 2001.)

value of 3.2°C, a 90 percent probability that ΔT_{2X} is over 2.2°C, and a 10 percent probability that ΔT_{2X} is greater than 5.0°C. The difference at the high end of climate sensitivity for these two pdfs has a huge impact on the likelihood that we will be able to avoid dangerous climate changes in the future.

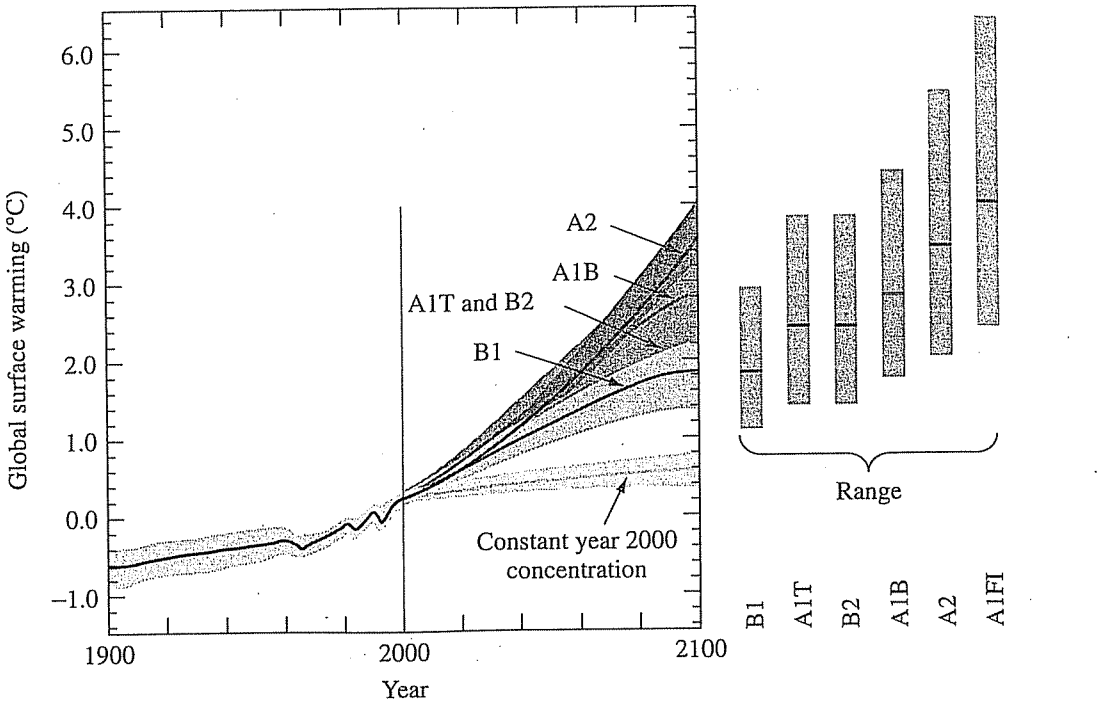

FIGURE 8.40 IPCC estimates of future global average surface warming relative to 1980 to 1999 for the six SRES scenarios. The gray bars to the right show best estimates and likely ranges for each scenario.
(*Source:* MTI-M, 2006.)

Figure 8.40 shows simulations of global average surface temperature for the six SRES scenarios. According to these 2007 simulations, a mean global warming between 2.4° and 4.4°C relative to mid-nineteenth-century levels is likely. Anywhere within that range would make the planet warmer than it has been for hundreds of thousands of years.

Dangerous Anthropogenic Interference with Climate

The United Nations Framework Convention on Climate Change calls for the "stabilization of greenhouse gas concentrations in the atmosphere at a level that would prevent *dangerous anthropogenic interference* (DAI) with the climate system" (UNFCC, 1992). Note the difference between stabilizing the rate at which carbon is emitted and stabilizing its concentration in the atmosphere. In fact, with a constant carbon emission rate at the current level, the equivalent carbon dioxide level would likely be double the preindustrial concentration of 280 ppm by 2100. Moreover, even if we stabilize the concentration of greenhouse gases in the atmosphere, it will take decades for the climate system to adjust to its new equilibrium temperature.

One way to begin thinking about dangerous climate change is to outline the sorts of impacts that global warming could have. The IPCC has done that, and their list of likely impacts in the relatively short term includes more frequent heat waves such as the one experienced in Europe in 2003, responsible for 35,000 deaths; more frequent intense storms like Katrina in 2005, leading to more extreme flooding and a surge in property damage; drier summers and increased risk of severe droughts with accompanying loss of farm productivity, especially in mid-latitude areas such as the

Mediterranean, Central America, and Southern Africa; less snow and reduced glacial extent, impacting areas that rely on snowmelt for water supply such as China, India, and Peru; sea-level rise and increased risk of coastal flooding that would displace millions of people in areas such as China, Bangladesh, and Egypt; and increasing ocean acidity as carbon dioxide is absorbed and converted to carbonic acid, leading to widespread impacts on marine ecosystems and biodiversity.

In the longer term, future warming could cause large-scale, potentially rapid and nonlinear climate responses, including the deglaciation of polar ice sheets, such as those in Greenland and West Antarctica, which could lead to several meters of sea level rise above that already expected due to thermal expansion of the oceans. Some climate changes could be nonlinear, producing responses that cause the climate system to jump from one stable state to another, as would occur if the North Atlantic thermohaline circulation system were to collapse (more on this later).

The question then arises as to how likely those impacts will become as a function of global temperatures increases. We have already seen the introduction of probability density functions in the context of the climate sensitivity factor. Some have tried to link probabilities to avoiding dangerous anthropogenic interference with climate. One such study shown in Figure 8.41 combines a number of assessments of the likelihood of exceeding the 2°C temperature rise thought to be capable of everything from widespread coral bleaching to disintegration of the Greenland ice sheet and perhaps a collapse of the West Antarctic ice sheet. As shown, a number of studies suggest that the stabilized CO_2-eq concentration needs to remain below about 450–500 ppm for the odds to be in favor of not exceeding a 2°C temperature rise.

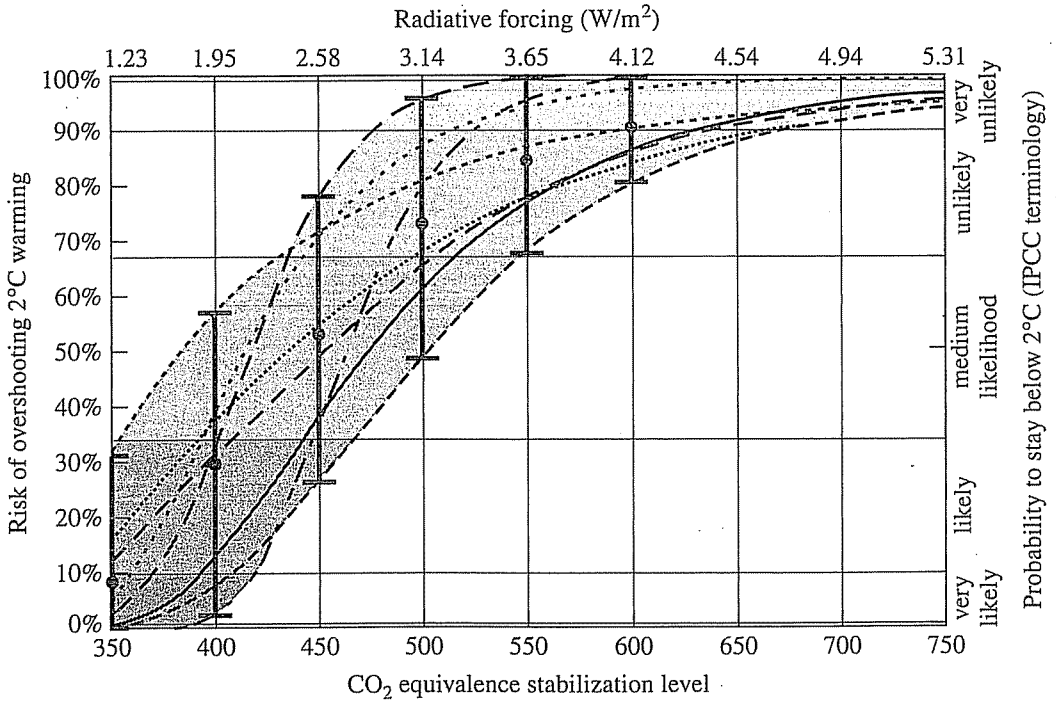

FIGURE 8.41 Estimated risks of exceeding a 2°C global mean temperature rise depending on the stabilized equivalent-CO_2 concentration. For example, if CO_2-eq stabilizes at 550 ppm (doubling of preindustrialized levels), the risk of overshooting a 2°C warming appears to be above 70 percent. Dotted and dashed lines correspond to different studies.
(*Source:* Meinhausen and den Elzen, 2004.)

8.11 Stabilizing Greenhouse Gases

The warning provided by studies of the likelihood of dangerous anthropogenic interference with climate increases our awareness of the need for mitigation strategies to help control greenhouse gas emissions. Since greenhouse gases accumulate in the atmosphere, to stabilize their concentration, we must do more than simply hold their emission rates constant. They need to be reduced to the point where their rate of addition to the atmosphere equals the rate at which they are removed. Figure 8.42 shows how emissions would have to decrease for the atmospheric concentration of CO_2 to stabilize at various levels. Notice avoiding dangerous anthropogenic interference would require emissions to start declining within the next 30 to 40 years.

Figure 8.43 suggests mitigation approaches that can contribute to reducing fossil-fuel carbon dioxide emissions. It consists of a reference emission scenario as a

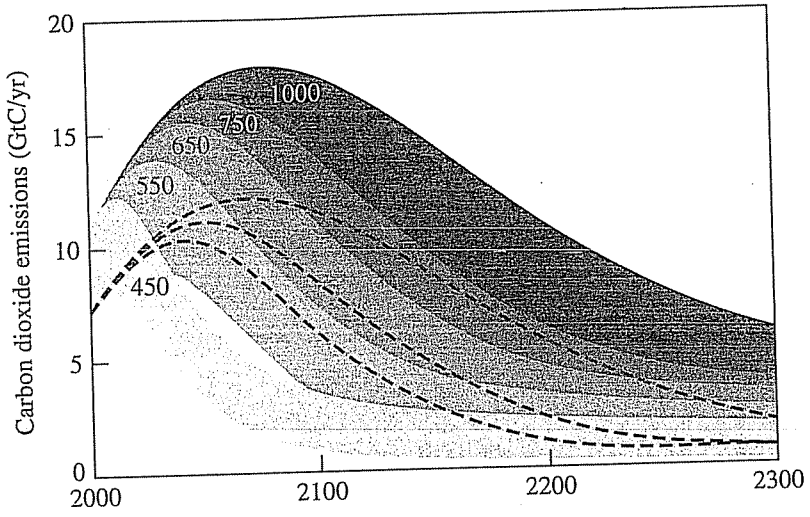

FIGURE 8.42 Pathways to climate stabilization. The numerical values refer to the eventual CO_2 (ppm) stabilization level achieved.
(*Source:* IPCC, 2001.)

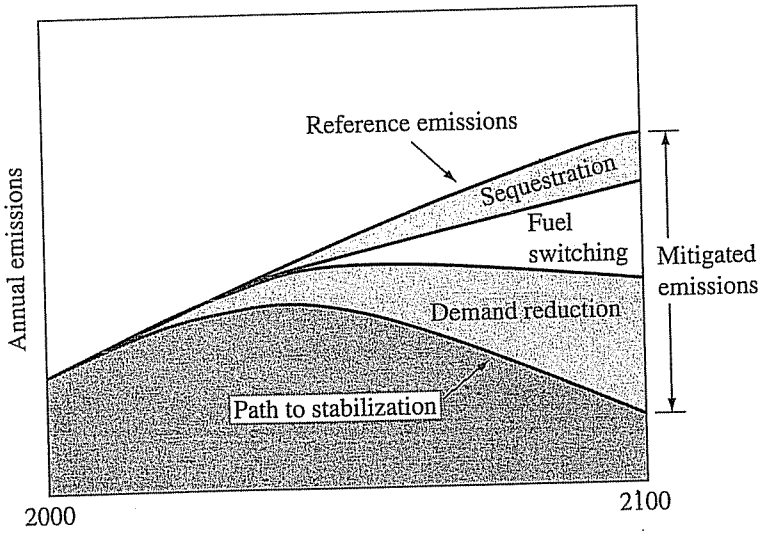

FIGURE 8.43 An example of a mitigation strategy for reducing fossil-fuel carbon dioxide emissions from a reference scenario to a stabilization path.

starting point, a target emission rate that would lead to the goal of climate stabilization, and an array of mitigation techniques that could be used to achieve that stabilization goal. Approaches to mitigation of carbon dioxide include *demand reduction* by increasing the efficiency with which we use energy and/or structural changes in the economy (e.g., a shift from manufacturing to a more service-oriented economy); *fuel switching,* which includes shifting from one fossil fuel to another (e.g., coal to natural gas) as well as increasing generation from nonfossil-fuel sources (e.g., nuclear, wind, solar, biomass, geothermal, and hydro); and *sequestration,* which includes carbon capture and storage (CCS) at power plants as well as increased sequestration in biomass.

An intuitively persuasive way to frame the problem of controlling future carbon emissions was introduced by Pacala and Socolow (2004). The concept is simple. Their reference scenario is in essence a 50-year projection of current carbon emission growth rates from 7 GtC/yr in 2005 to 14 GtC/yr in 2055, which makes it quite similar to the SRES B2 scenario. Their mitigation goal is to at least hold emissions constant at 7 Gt/yr over that 50-year period. To do so would require the elimination of 175 GtC of emissions over the next 50 years, which is the area of the emissions stabilization triangle shown in Figure 8.44.

As shown in Figure 8.45, they then proceed to break that emissions triangle into seven *stabilization wedges,* with each wedge having the ability to eliminate 1 GtC/yr in 2055. The Princeton Carbon Mitigation Initiative is in the process of identifying a significant number of strategies already available that could reduce emissions equivalent to one wedge of carbon emissions if deployed on a large scale. Their list includes the following:

1. Double the fuel efficiency of every automobile by 2050.
2. Drive half as many miles.
3. Utilize the best efficiency practices for all residential and commercial buildings.
4. Double the efficiency of coal-fired power plants.
5. Using natural gas instead of coal at 1,400 power plants.

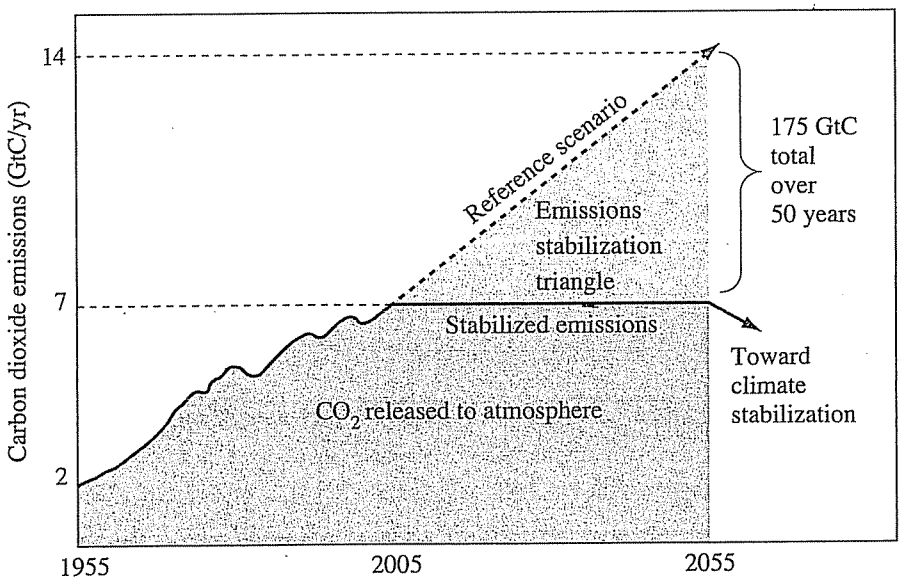

FIGURE 8.44 A 50-year emissions stabilization scenario. (*Source:* Pacala and Socolow, 2004.)

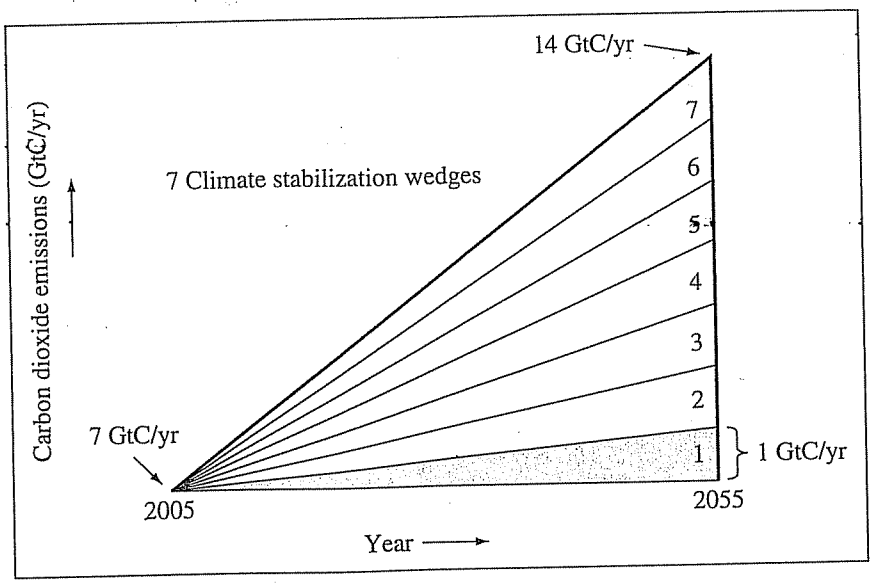

FIGURE 8.45 Each stabilization wedge eliminates 1 GtC/yr by 2055. (*Source:* Pacala and Socolow.)

6. Capture and store carbon emissions from 800 coal-fired power plants.
7. Triple the current nuclear power generation capacity.
8. Increase existing wind turbine capacity by a factor of 50.
9. Use 4 million wind turbines to produce hydrogen fuel.
10. Install 700 times the existing solar power capacity.
11. Increase ethanol production by a factor of 50 using cellulosic sources.
12. Eliminate tropical deforestation and double the rate of new forest planting.
13. Increase soil conservation tillage in all agricultural soils.
14. Capture and store carbon from 180 coal-based synfuels plants.
15. Increase hydrogen fuel production from fossil-fuel sources by a factor of 10.

Every one of these options is already available on a commercial scale. Full deployment of seven of them offers the enticing potential to at least stabilize emissions over the next half century. Realize, of course, that stabilizing emissions does not stabilize the concentrations of greenhouse gases in the atmosphere, and to avoid dangerous anthropogenic interference with our climate system, we must do much better than that.

8.12 The Oceans and Climate Change

The oceans cover 70 percent of the Earth's surface and contain over 97 percent of the Earth's water. They have high heat capacity, so they warm slowly, and their currents distribute heat around the globe, greatly affecting local and regional temperatures on the land. They store 50 times as much carbon as the atmosphere, and they exchange carbon dioxide back and forth across the atmosphere-ocean interface at a rate that dwarfs the contribution by humankind. In other words, the oceans significantly affect and are affected by climate change. Greenhouse enhancement can affect the

ocean in many ways, but three of the most important changes have to do with ocean acidification, rising sea levels, and changes in the ocean circulation. In addition, biological processes that result in the removal of carbon from the atmosphere can be affected by climate change, and in turn, those changes can affect climate.

Ocean Acidification

The oceans are performing a great service to the climate system by absorbing so much of the carbon dioxide we continuously pump into the atmosphere. That absorption comes at a price, however, since it is causing subtle chemical changes in the oceans that may have enormous implications for marine ecosystems.

Recall from Chapter 3 that dissolved inorganic carbon exists in three forms: dissolved CO_2 gas, bicarbonate (HCO_3^-), and carbonate (CO_3^{2-}) ions. When CO_2 dissolves into sea water, some of it creates carbonic acid (H_2CO_3), which in turn ionizes to form hydrogen and bicarbonate:

$$CO_2 + H_2O \Leftrightarrow H_2CO_3 \Leftrightarrow H^+ + HCO_3^- \tag{8.44}$$

The bicarbonate ions (HCO_3^-), in turn, ionize to some extent into hydrogen and carbonate ions:

$$HCO_3^- \Leftrightarrow H^+ + CO_3^{2-} \tag{8.45}$$

The natural pH of the oceans is between 8.0 and 8.3, which means it is somewhat alkaline. The preceding reactions release hydrogen ions, which make the water more acidic (less alkaline) as CO_2 absorption increases. Studies have shown that the oceans have already experienced a drop in pH of about 0.1 since preindustrial times, and it seems likely ocean pH will fall by another 0.3 by the year 2100 (Caldeira and Wickett, 2003). If that happens, the oceans will be more acidic than they have been for hundreds of millions of years.

The preceding reactions proceed in both directions, and the resulting balance of aqueous CO_2, bicarbonate, and carbonate ions is a function of the pH (Figure 8.46). As Figure 8.46 shows, one consequence of a decrease in pH is that carbonate decreases as well. And carbonate is needed to build the calcium carbonate ($CaCO_3$)

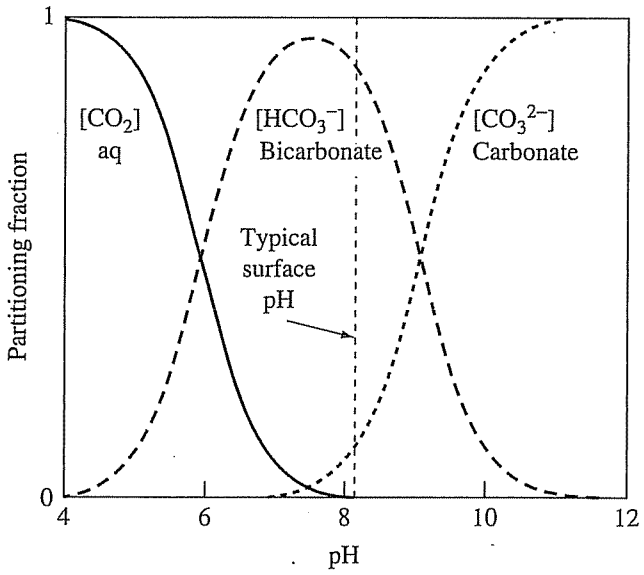

FIGURE 8.46 The relative proportions of dissolved CO_2, bicarbonate (HCO_3^-), and carbonate (CO_3^{2-}) depends on pH. When pH drops, less carbonate is available for calcifying organisms to grow and maintain calcium carbonate shells.

in shells and other hard parts of marine organisms. Some of the most important organisms likely to be affected by a lack of carbonate are certain types of plankton and small marine snails that are a major source of food for fish and marine mammals, including some species of whales. Coral reefs would also be affected since they are built from secretions of calcium carbonate by small sea anemone-like animals and coralline algae, which colonize and literally create the reefs.

Another impact of the drop in carbonate ions in seawater is the increased potential for shells to literally dissolve. The balance between the rate at which solid calcium carbonate dissociates and the rate at which it is formed is related to the concentration of carbonate ions:

$$CaCO_3 \Leftrightarrow Ca^{2+} + CO_3^{2-} \tag{8.46}$$

With less carbonate, the reaction shifts to the right, increasing the tendency for calcium carbonate to dissolve. The dissociation constant that goes with (8.46) is temperature and pressure dependent, and in cold, deep waters, the shift is sufficient to dissolve calcium carbonate shells. There is a depth, called the *saturation horizon*, below which shells dissolve and above which they survive. With more atmospheric CO_2, the shift in pH and carbonate has caused the saturation horizons to shift closer to the surface, in some areas by as much as 50 to 200 meters compared to where they were in the 1800s. Thinning of the shell-friendly, upper layer of the oceans, with unknown consequences, is a rising concern for climate and marine scientists trying to predict the impacts of global warming.

Rising Sea Level

Water expands as it warms, decreasing its density and increasing its volume, which causes sea level to rise. In addition, melting glaciers and ice caps contribute to increasing ocean volume and rising sea levels. Thermal expansion is the primary cause of the current 3 mm per year rise in sea level, but melting glaciers have the potential to accelerate that rise substantially in the future.

Almost all of the world's nonoceanic water is stored in ice caps and glaciers, and almost all of that is contained in just two great ice sheets—the Antarctic ice sheet and the Greenland ice sheet. Table 8.9 shows the volume of ice in these ice sheets plus the remaining ice stored in glaciers and ice caps along with the equivalent rise in sea level that complete melting could incur. As shown there, the Antarctic ice sheet stores enough water to raise the level of the oceans by 73 meters.

The Antarctic ice sheet is projected to grow slightly in the future due to increased precipitation coupled with extremely cold temperatures, so it may not

TABLE 8.9

Some Characteristics of the World's Ice

	Area (10^6 km^2)	Volume (10^6 km^3)	Sea Level Equivalent (m)
Antarctic ice sheet	12.1	29	73
Greenland ice sheet	1.71	2.95	7.4
Glaciers and ice caps	0.64	0.1 ± 0.02	0.3 ± 0.05

Source: IPCC, 1995.

contribute to rising sea levels. A portion of Antarctic ice, however, rests on the ocean floor, and there has been some concern that if that West Antarctic Ice Sheet (WAIC) were to break loose and slide into the ocean, it could cause a rapid rise in sea level of perhaps 5 or 6 meters. Indeed, a 200-m thick, 3,200 km^2 chunk of the Larsen Ice Shelf did collapse into the sea in 2002, amplifying concern that ocean warming and the acceleration of ice flows may be destabilizing the ice sheet that could cause a runaway discharge into the oceans. Some studies indicate a critical threshold for WAIC collapse might be in the range of a 2°C to 5°C global temperature rise, but too many uncertainties remain to be confident that this is an accurate estimate.

Inland portions of the Greenland ice sheet have shown a slight increase in volume, but significant melting is occurring along the coasts. Meltwater seeping down through the crevices of the melting ice seems to be acting as a lubricant that is accelerating glacial movement toward the ocean. There is great concern for a potential tipping point, beyond which the surface temperature of the ice sheet will become too warm to allow winter glacial growth to offset summertime melting. At that point, which is estimated by some to be a 2 to 3°C mean global temperature increase above preindustrial levels, the Greenland ice sheet will begin to melt irreversibly.

Atmospheric-ocean coupled general circulation models have been used to estimate future sea-level change for a great many SRES scenarios. For the illustrative A1B and B2 scenarios shown in Figure 8.47, a sea level rise on the order of one quarter of a meter by 2100 is projected. Multiple variations on all of the SRES scenarios show much wider variation, with most lying somewhere between 0.2 to 0.7 meters in 2100. The enormous thermal capacitance of the oceans means that sea level will continue to rise well beyond the time when carbon dioxide concentrations stabilize in the atmosphere as the oceans slowly adjust to the increased radiative forcing.

Rising sea levels coupled with the projected increase in the fraction of hurricanes and storms that are predicted to be highly dangerous may result in large areas of densely populated coastline having to be abandoned. With approximately 20 percent

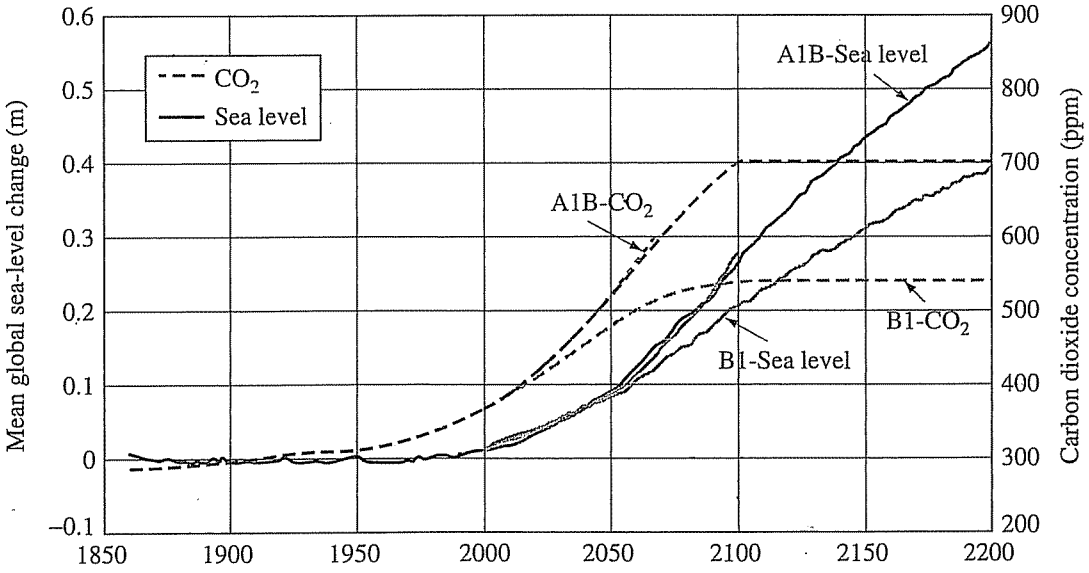

FIGURE 8.47 Sea-level rise and CO_2 concentrations for illustrative SRES scenarios A1B and B2.
(*Source:* Max Planck Institute-Meteorology, 2006.)

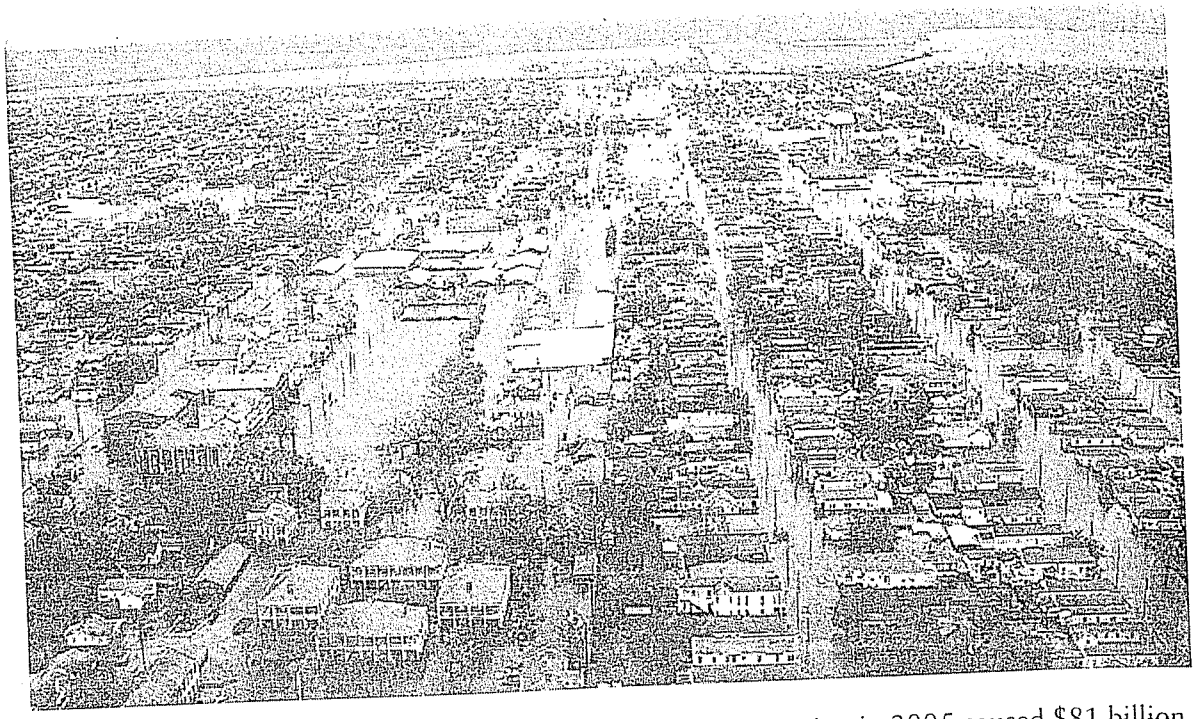

FIGURE 8.48 Flooding in New Orleans after Hurricane Katrina in 2005 caused $81 billion in damages and 1,800 deaths.

of the world's population living within 30 km of a coastline, tens of millions of people may become climate change refugees. Damage due to storm surges could be devastating to coastal areas that have not been adequately fortified, which places an added burden on countries that don't have the resources to adapt to rising water levels. Hurricane Katrina (Figure 8.48), which slammed into the Gulf Coast in 2005, provided a stark example of how costly, both in terms of human lives (over 1,800 deaths) and property damage (over $80 billion), storm events can be. Other potential impacts of rising sea levels include increased shoreline erosion, exacerbated coastal flooding, inundation of coastal wetlands, and increased salinity of estuaries and aquifers.

Thermohaline Circulation and the Biological Carbon Pump

Atmospheric carbon dioxide is absorbed by the oceans and forms inorganic dissolved bicarbonate and carbonate ions. A small fraction of that carbon is taken up by phytoplankton during photosynthesis and becomes part of the food chain in the upper layer of the oceans (the euphotic zone). Photosynthesis, respiration, and decomposition taking place in the surface layers of the ocean remove and replace some 40 to 50 GtC per year. There is a net removal, however, of about 10 GtC per year (nearly twice the carbon emission rate from the combustion of fossil fuels) from the surface waters as dissolved organic carbon, particulate carbon, and $CaCO_3$ in the "hard" parts of marine algae and animals sink into the intermediate and deep ocean. That removal process is known as the *biological carbon pump*.

Related to the biological pump is another process called the *thermohaline circulation* system, or sometimes the *Atlantic conveyor*, that transports carbon-rich surface waters into the deep oceans. As shown in Figure 8.49, there is an enormous

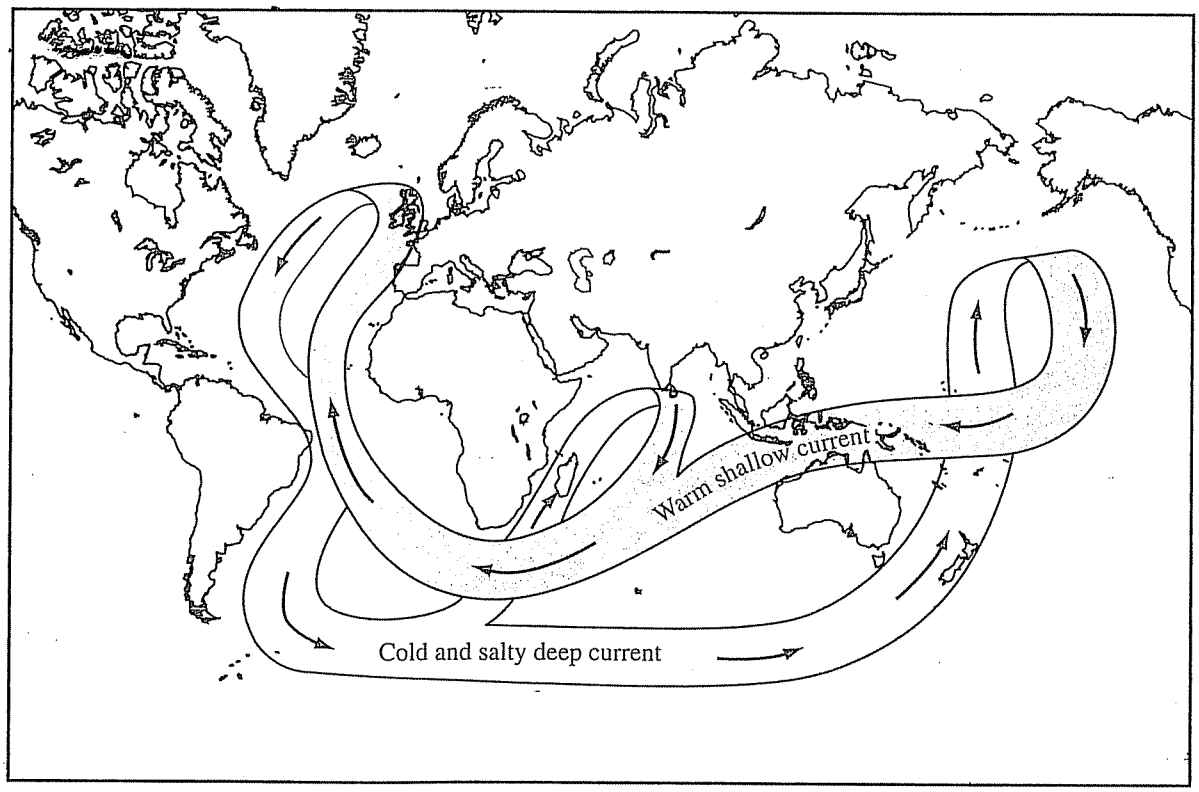

FIGURE 8.49 The thermohaline circulation system is driven by cold, salty water sinking into the North Atlantic abyss and upwelling near India and in the Pacific.

flow of ocean water around the globe, equal to the combined flow of all the world's rivers, that transports heat and nutrients from one place to another. Relatively warm seawater near the surface flows into the North Atlantic, where winds encourage evaporation and help sweep the surface waters aside, allowing the warm subsurface water to rise. That rising warm water gives off an enormous amount of heat as it reaches the surface. It is this source of heat that accounts for Western Europe's relatively mild winters. As that warm surface water evaporates and cools, it becomes more salty and dense, eventually becoming so dense that it sinks down to the ocean bottom. That North Atlantic deep water then moves southward, around the southern tip of Africa. Some emerges off the coast of India, but most upwells in the Pacific ocean where it starts its path back to the North Atlantic.

What makes the thermohaline circulation especially important in studies of climate change is the fact that it appears to have several stable states. It runs at a fast rate, an extremely slow rate, or at its present rate, which is somewhere in the middle. The transition between those stable states can occur in a relatively few years. Shifting from one stable state to another is thought to be responsible for a rather dramatic climate shift that occurred in northern Europe just after the last glacial period ended. Some 11,000 years ago, while glaciers were retreating and temperatures were back to interglacial levels, northern Europe and northeastern North America suddenly plunged back into glacial conditions. The temperature in Greenland dropped by 6°C in less than 100 years, stayed that way for 1,000 years, then jumped back to warm conditions in about 20 years (Broeker and Denton, 1990). The explanation for this event, known as the *Younger Dryas* (named for an Arctic flower that grew in Europe during this period), is based on the sudden stopping, then restarting

1,000 years later, of the Atlantic conveyor. Apparently, glacial meltwater draining from the North American ice sheet into the North Atlantic diluted the salty surface water enough to halt the density-driven dive into the abyss, which stopped the entire conveyor. Europe lost the warming influence of the current, and glacial conditions suddenly returned.

Most coupled ocean-atmosphere models show a future decrease in the strength of the Atlantic conveyor, which on its own would lead to some cooling of Europe and the east coast of the United States. That cooling would offset some but not all of the projected regional warming that would otherwise be expected due to an enhanced greenhouse effect. The possibility of a complete collapse of thermohaline circulation that could result if precipitation and runoff patterns change sufficiently is another of the potential "surprises" that worry some climatologists.

8.13 | Changes in Stratospheric Ozone

The changes occurring in the stratosphere's protective layer of ozone are closely linked to the greenhouse problem just discussed. Many of the same gases are involved, including CFCs, halons, methane, and nitrous oxide, as well as aerosols and ozone itself. Some of the gases that enhance the greenhouse effect, such as methane, actually reduce stratospheric ozone depletion, so the two problems really must be considered together.

Ozone has the unusual characteristic of being beneficial when it is in the stratosphere protecting us from exposure to ultraviolet radiation, while ozone formed near the ground in photochemical smog reactions is, as we have seen in Chapter 7, harmful to humans and other living things. About 90 percent of the atmosphere's ozone is contained in the stratosphere between roughly 10 and 50 km in what is commonly referred to as the *ozone layer*. The remaining 10 percent or so is contained in the troposphere, near the ground, above cities and industrialized areas. Figure 8.50 shows this distribution of ozone in the atmosphere along with some comments on its beneficial and harmful attributes.

If all of the atmospheric ozone overhead at any given spot on the Earth were to be brought down to ground level so that it would be subjected to 1 atm of pressure, it would form a layer only a few millimeters thick. In fact, one of the common methods of expressing the total amount of ozone overhead is in terms of *Dobson units* (DU), where 1 DU is equivalent to a layer of ozone 0.01 mm thick at 1 atm of pressure at 0°C. At midlatitudes, the ozone overhead is typically about 350 DU (3.5 mm at 1 atm); near the equator, it is closer to 250 DU. During the annual appearance of the ozone hole over Antarctica, the ozone column drops below 100 DU.

The Ultraviolet (UV) Portion of the Solar Spectrum

Ozone (O_3) is continuously being created in the stratosphere by photochemical reactions powered by short-wavelength ultraviolet (UV) radiation, while at the same time it is continuously being removed by other photochemical reactions that convert it back to diatomic oxygen molecules (O_2). The rates of creation and removal at any given time and location dictate the concentrations of ozone present.

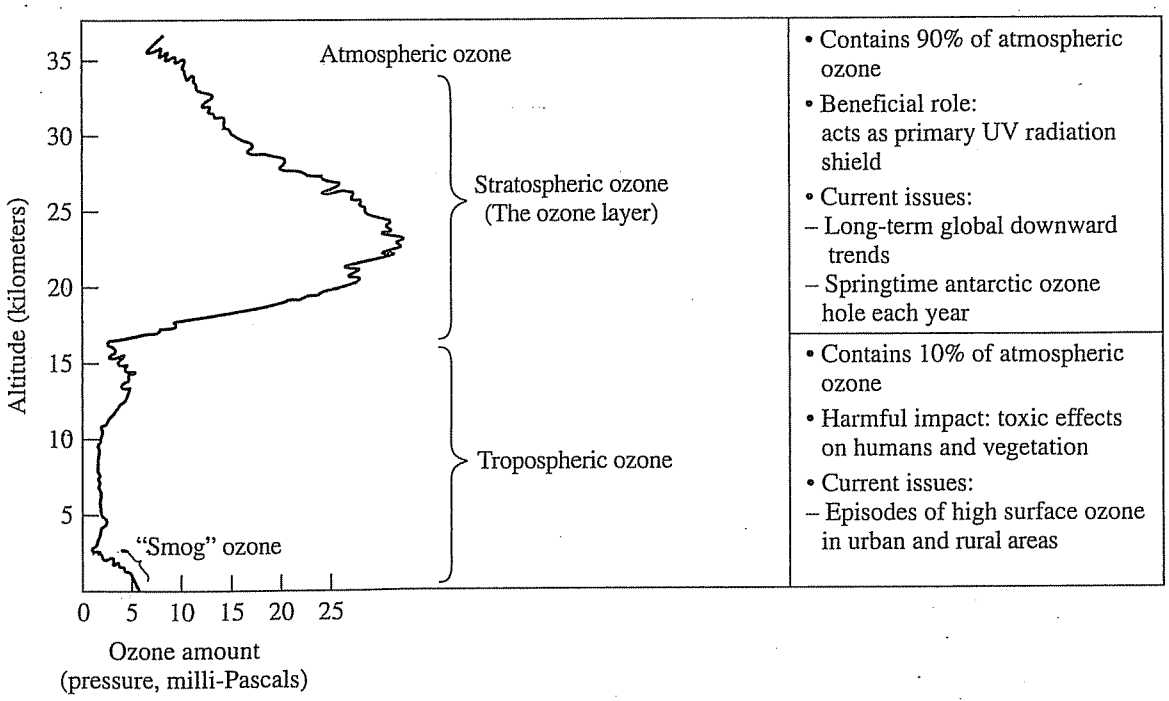

FIGURE 8.50 Amounts of ozone in the troposphere and stratosphere, including comments on the beneficial and harmful roles it plays in each region.
(*Source:* UNEP, 1994.)

The energy required to drive some of these photochemical reactions comes from sunlight penetrating the atmosphere. As you may recall, it is convenient to consider such electromagnetic radiation in some contexts as a wave phenomenon and in others as a packet of energy called a photon. The energy content of a single photon is the proportional to its frequency, and inversely proportional to its wavelength:

$$E = h\nu = \frac{hc}{\lambda} \tag{8.47}$$

where

E = the energy of one photon (J)
h = Planck's constant (6.626218×10^{-34} J s)
c = the speed of light (2.997925×10^{8} m/s)
ν = frequency (s^{-1})
λ = wavelength (m)

Thus, photons with shorter wavelengths have higher energy content.

The entire solar spectrum was introduced in Figure 8.10, where it was used to help derive the effective temperature of the Earth. In the context of stratospheric ozone depletion, however, it is only the UV portion of the spectrum that is of interest. Photons associated with those shorter wavelengths can have sufficient energy to break apart molecules, initiating *photochemical reactions*. Molecules that are dissociated by UV light are said to have undergone *photolysis*.

The energy required to drive photochemical reactions is often expressed as an amount of energy per mole of gas under standard conditions. If we assume the energy required under stratospheric conditions is not much different, we can easily derive

the maximum wavelength that a photon must have to cause photolysis. A single photon (with sufficient energy) can cause photolysis in one molecule. And since there are Avogadro's number (6.02×10^{23}) of molecules in one mole of gas, we can convert energy needed per mole into the energy that one photon must have, as follows:

$$E(\text{J/photon}) = \frac{E(\text{J/mol})}{1 \text{ photon/molecule} \times 6.02 \times 10^{23} \text{ molecule/mol}} \tag{8.48}$$

Now we can use (8.47) to solve for the wavelength.

EXAMPLE 8.13 Photon Energy for Photolysis

What is the maximum wavelength that a photon can have to photodissociate diatomic oxygen if 495 kJ/mol are required?

$$O_2 + h\nu \rightarrow O + O$$

Solution The energy that a photon must have is given by (8.48):

$$E = \frac{495 \text{ kJ/mol} \times 10^3 \text{ J/kJ}}{1 \text{ photon/molecule} \times 6.02 \times 10^{23} \text{ molecule/mol}} = 8.22 \times 10^{-19} \text{ J/photon}$$

Rearranging (8.46) and substituting the energy that the photon must have gives us

$$\lambda_{max} = \frac{hc}{E} = \frac{6.626 \times 10^{-34}(\text{Js}) \cdot 2.998 \times 10^8(\text{m/s})}{8.22 \times 10^{-19} \text{ J}} = 241.6 \times 10^{-9} \text{m}$$
$$= 241.6 \text{ nm}$$

Thus, photons with wavelengths longer than 241.6 nm will not have sufficient energy to break apart the oxygen molecule.

The wavelengths that are most important in the context of stratospheric ozone depletion are in the 100 to 400 nm portion of the ultraviolet (UV) spectrum. It is called ultraviolet since wavelengths just above 400 nm are violet in color and visible to the human eye. For analogous reasons, wavelengths above 700 are called infrared, since 700 nm is the edge of the red portion of the visible spectrum. The most important portion of the UV spectrum is divided into three regions, designated as UV-A, UV-B, and UV-C, which have wavelengths as shown in Figure 8.51.

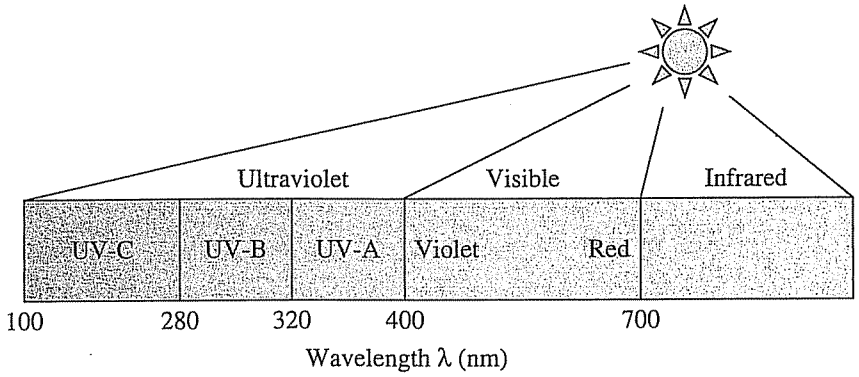

FIGURE 8.51 The ultraviolet (UV), visible, and infrared (IR) portions of the solar spectrum, including the biologically important UV-A, UV-B, and UV-C regions.

About 99 percent of the incoming solar UV that makes it through the atmosphere is UV-A (320 to 400 nm). It is sometimes referred to as "black light" since it is invisible to the human eye, though some animals can use it for vision. UV-A penetrates deeply into human skin, causing tanning (but little skin reddening), DNA damage, photoaging (toughening of the skin, wrinkles), and possibly skin cancer. Some exposure to UV-A benefits human health by helping to induce the formation of vitamin D. UV-B radiation (280–320 nm) poses the greatest danger to human health. It causes reddening of the skin (erythema) and reduction of vitamin-D synthesis in the short term; in the long term, it is a cause of skin cancer, cataracts, and suppression of the immune system. The "SPF rating" of sunscreen products refers to their ability to protect us from UV-B. Some sunscreens now include ingredients that also help block UV-A. Photons within the UV-C portion of the spectrum (100 to 280 nm) readily destroy DNA, which makes them extremely dangerous but also lets artificially created UV-C be used as a very effective disinfectant for water treatment and other germicidal applications. Fortunately, the atmosphere effectively shields us from these very potent photons.

The Ozone Layer as a Protective Shield

Ozone formation in the stratosphere can be described by the following pair of reactions. In the first, atomic oxygen (O) is formed by the photolytic decomposition of diatomic oxygen (O_2).

$$O_2 + h\nu \rightarrow O + O \tag{8.49}$$

where $h\nu$ represents a photon. As shown in Example 8.13, for this dissociation to take place, the photon must have a wavelength of no more than 242 nanometers. Photons with less energy (longer wavelengths) cannot cause the reaction to take place; all they can do is heat up the molecule that absorbs them. Photons with higher energy than the minimum required use some of their energy to cause photolysis, and what is left over is dissipated as heat. Diatomic oxygen (O_2) has its maximum absorption at about 140 nm, and it is a very effective absorber of UV-C radiation between 130 and 180 nm.

The atomic oxygen formed by (8.49) reacts rapidly with diatomic oxygen to form ozone,

$$O + O_2 + M \rightarrow O_3 + M \tag{8.50}$$

where M represents a third body (usually a nearby N_2 molecule) needed to carry away the heat generated in the reaction.

Opposing the preceding ozone formation process is ozone removal by photodissociation:

$$O_3 + h\nu \rightarrow O_2 + O \tag{8.51}$$

The absorptance of ozone extends from about 200 to 320 nm and reaches its peak at 255 nm. The reaction shown in (8.51) is very effective in removing UV-C radiation and some of the UV-B before it reaches the Earth's surface.

The preceding combination of reactions (8.49 to 8.51) forms a chain in which oxygen atoms are constantly being shuttled back and forth between the various molecular forms. A principal effect is the absorption of most of the short-wavelength, potentially damaging, UV radiation as it tries to pass through the stratosphere.

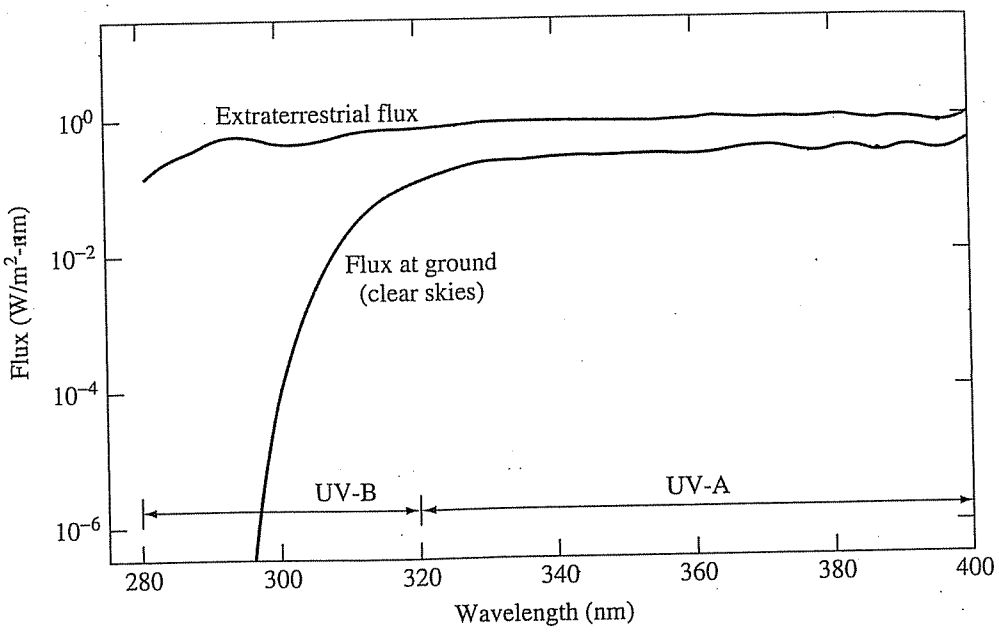

FIGURE 8.52 Extraterrestrial solar UV flux and expected flux at the Earth's surface on a clear day with the sun 60° from the zenith.
(*Source:* Frederick, 1986.)

In addition, that absorption also heats the stratosphere, causing the temperature inversion shown earlier in Figure 8.1. That temperature inversion, which is what defines the stratosphere, produces stable atmospheric conditions that lead to long residence times for stratospheric pollutants.

The effectiveness of these reactions in removing short-wavelength UV is demonstrated in Figure 8.52, in which the extraterrestrial solar flux and the flux actually reaching the Earth's surface are shown. The radiation reaching the surface has been drawn for a clear day with the sun assumed to be 60° from the zenith (overhead), corresponding roughly to a typical mid-latitude site in the afternoon. As can be seen, the radiation reaching the Earth's surface is rapidly reduced for wavelengths less than about 320 nm. In fact, an intact ozone layer shields us from almost all of the UV having wavelengths shorter than about 290 nm.

Catalytic Destruction of Stratospheric Ozone

As is now common knowledge, the natural formation and destruction of ozone in the stratosphere is being affected by gases that we release into the atmosphere. In particular, ozone destruction is enhanced by catalytic reactions that can be represented as follows:

$$\begin{aligned} X + O_3 &\rightarrow XO + O_2 \\ \text{and} \quad XO + O &\rightarrow X + O_2 \\ \hline \text{for a net} \quad O + O_3 &\rightarrow 2\,O_2 \end{aligned} \qquad (8.52)$$

where X is a free radical such as Cl, Br, H, OH, or NO (recall that free radicals are highly reactive atoms or molecules that have an odd number of electrons, which means one electron is not paired with another atom). Notice in (8.52) how the X radical that enters the first reaction is released in the second, freeing it to go on and participate in another catalytic cycle. The net result of the preceding pair of

reactions is the destruction of one ozone molecule. The original catalyst that started the reactions, however, may go on to destroy thousands more ozone molecules before it eventually leaves the stratosphere.

Chlorofluorocarbons (CFCs) are a major source of ozone-destroying chlorine. Recall that CFCs have long atmospheric lifetimes since they are inert and nonwater-soluble, so they aren't removed in the troposphere by chemical reactions or rainfall. Eventually, CFCs drift into the stratosphere, where they are exposed to UV radiation, which breaks apart the molecules, freeing the chlorine. CFCs typically require photons in the UV-C range with wavelengths shorter than 220 nm for photolysis. For example, CFC-12, which has an atmospheric lifetime of 100 years (Table 8.7), undergoes photolysis as follows:

$$CF_2Cl_2 + \text{UV-C} \rightarrow CF_2Cl + Cl \tag{8.53}$$

Eventually the second chlorine atom is also released. The freed chlorine then acts as a catalyst as described by (8.52):

$$\begin{aligned} Cl + O_3 &\rightarrow ClO + O_2 \\ ClO + O &\rightarrow Cl + O_2 \\ \text{Net:}\quad O + O_3 &\rightarrow 2\,O_2 \end{aligned} \tag{8.54}$$

The chlorine atom makes this loop tens of thousands of times, but eventually it reacts with methane to become water-soluble HCl that can diffuse into the troposphere, where it can be washed out of the atmosphere by rainfall.

$$Cl + CH_4 \rightarrow HCl + CH_3 \tag{8.55}$$

Chlorine that has been incorporated into HCl, as in (8.55), is *inactive;* that is, it does not participate in the catalytic destruction of ozone represented by (8.54). Notice that methane, which is a potent greenhouse gas, helps remove the ozone-destroying, active form of chlorine from the stratosphere. In the context of climate change, methane is part of the problem; in the context of ozone depletion, it is part of the cure.

Another way that chlorine is removed from the catalytic chain reaction is by its incorporation into chlorine nitrate, $ClONO_2$:

$$ClO + NO_2 \rightarrow ClONO_2 \tag{8.56}$$

At any given time, as much as 99 percent of the chlorine in the stratosphere is tied up in these inactive molecules, HCl and $ClONO_2$. Unfortunately, those inactive molecules are subject to chemical reactions and photolysis that can restore the chlorine to its active forms, Cl and ClO, especially when there are nearby particles available that provide platforms upon which the reactions can take place. Sulfate aerosols, especially from volcanic eruptions, and clouds of nitric acid ice over the Antarctic provide such surfaces. When gases and particles are both involved, the chemistry is referred to as *heterogeneous* reactions, as opposed to *homogeneous* reactions involving gases alone.

Bromine in the stratosphere is another potent ozone-depleting gas, as the following reactions suggest:

$$\begin{aligned} Br + O_3 &\rightarrow BrO + O_2 \\ BrO + ClO &\rightarrow Br + ClO_2 \end{aligned} \tag{8.57}$$

As is the case with chlorine, bromine acts as a catalyst destroying ozone until it eventually combines with methane to form hydrogen bromide (HBr). Hydrogen bromide deactivates the bromine, but not for long. Photolysis rather quickly decomposes HBr, sending bromine back into its catalytic loop with ozone. In this regard, bromine is much more potent than chlorine since stratospheric chlorine exists mostly in its inactive forms, HCl and $ClONO_2$.

The main source of bromine in the stratosphere is methyl bromide (CH_3Br), about half of which comes from the oceans, and about half is due to anthropogenic sources. Methyl bromide is used extensively in agriculture to sterilize soil and fumigate some crops after they are harvested. Other anthropogenic sources include biomass burning and automobile exhaust emissions when leaded fuels are used. Bromine has also been used as a flame retardent in fire extinguishers.

The Antarctic Ozone Hole

Chlorine that has been incorporated into hydrogen chloride (HCl) or chlorine nitrate ($ClONO_2$) is inactive, so it doesn't contribute to the destruction of ozone. In the Antarctic winter, however, a unique atmospheric condition known as the *polar vortex* traps air above the pole and creates conditions that eventually allow the chlorine to be activated. The polar vortex consists of a whirling mass of extremely cold air that forms over the South Pole during the period of total darkness in the Antarctic winter. The vortex effectively isolates the air above the pole from the rest of the atmosphere until the Antarctic spring arrives in September. Stratospheric temperatures in the vortex may drop to below −90°C, which is cold enough to form polar stratospheric clouds (PSCs) even though the air is very dry. The ice crystals that make up polar clouds play a key role in the Antarctic phenomenon by providing reaction surfaces that allow chemical species to stay together long enough to react with each other.

A number of reactions take place on the surfaces of polar stratospheric cloud particles that result in the formation of chlorine gas (Cl_2). For example,

$$ClONO_2 + H_2O \rightarrow HOCl + HNO_3 \tag{8.58}$$

$$HOCl + HCl \rightarrow Cl_2 + H_2O \tag{8.59}$$

$$ClONO_2 + HCl \rightarrow Cl_2 + HNO_3 \tag{8.60}$$

Once the sun rises in the Antarctic spring in September, the chlorine gas (Cl_2) formed during the darkness of winter photolytically decomposes into atomic chlorine:

$$Cl_2 + h\nu \rightarrow 2\ Cl \tag{8.61}$$

which then destroys ozone by reinitiating the catalytic destruction process described in (8.54):

$$(Cl + O_3 \rightarrow ClO + O_2) + (ClO + O \rightarrow Cl + O_2) = O + O_3 \rightarrow 2\ O_2 \tag{8.62}$$

The destruction of ozone as the sun first appears in the Antarctic spring proceeds as described until the nitric acid (HNO_3) formed in (8.58) and (8.60) photolyzes and forms inactive chlorine nitrate ($ClONO_2$), which stops the ozone destruction process. As the vortex breaks down in the spring, ozone from nearby areas rushes in

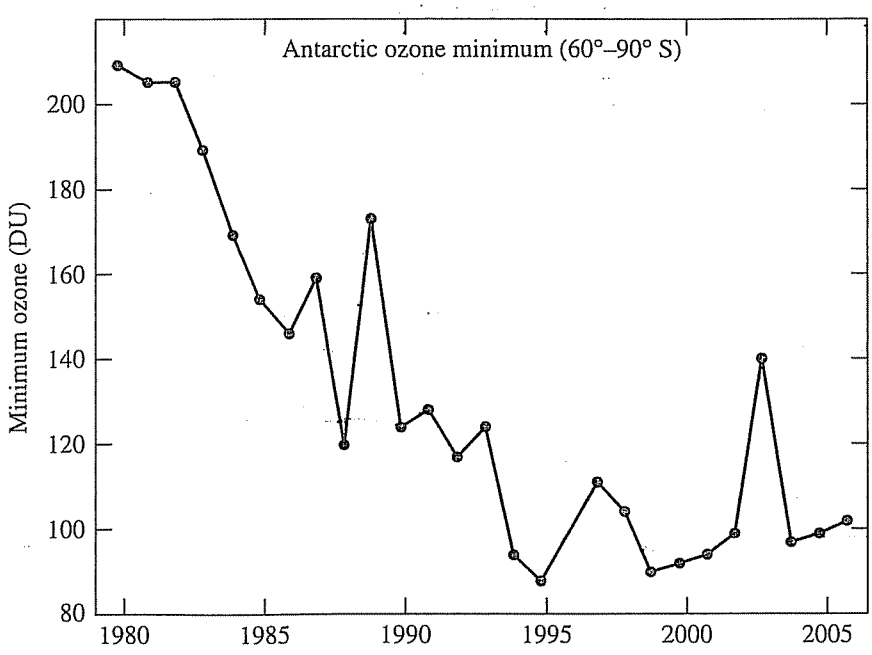

FIGURE 8.53 Antarctic ozone minimun (60°–90° S), suggesting the beginning of recovery in about the year 2000.
(*Source:* NASA Website.)

and replenishes the ozone above Antarctica. Conversely, the transport of ozone-depleted air from polar regions is thought to be contributing to decreases in stratospheric ozone at middle latitudes. The entire ozone-hole cycle typically lasts from mid-August until the end of November, reaching its greatest depth and aerial extent near the first of October.

Concern over possible destruction of stratospheric ozone was first expressed by two scientists, F. Sherwood Rowland and Mario J. Molina in 1974; however, it wasn't until 1985, with the dramatic announcement of the discovery of a "hole" in the ozone over Antarctica, that the world began to recognize the seriousness of the problem. In 1995, Rowland, Molina, and Paul Crutzen were awarded the Nobel Prize in Chemistry for their pioneering work in explaining the chemical processes that lead to the destruction of stratospheric ozone.

Figure 8.53 shows how deep the ozone hole has been over the past couple of decades. The values shown (in Dobson units) correspond to the minimum values measured anywhere within the hole each year. When measurements first began, in the early 1980s, those minimums were a little above 200 DU. They reached their lowest level in 1995 (88 DU) and now seem to be somewhat on the rise as efforts to control emissions of ozone-depleting substances begin to have effect. The area of the ozone hole has shown a similar pattern to the depth (Figure 8.54). The hole grows in area to about 25 million km^2 in late September, making it roughly equivalent in size to the entire North American continent.

The very low stratospheric temperatures over Antarctica, which form those polar stratospheric clouds, are not duplicated in the Arctic. The combination of land and ocean areas in the Arctic results in warmer temperatures and much less of a polar vortex, factors that do not encourage the formation of polar clouds. The result is a much less dramatic thinning of the ozone layer over the Arctic in the spring, although it is still significant. There is concern, however, that greenhouse effect

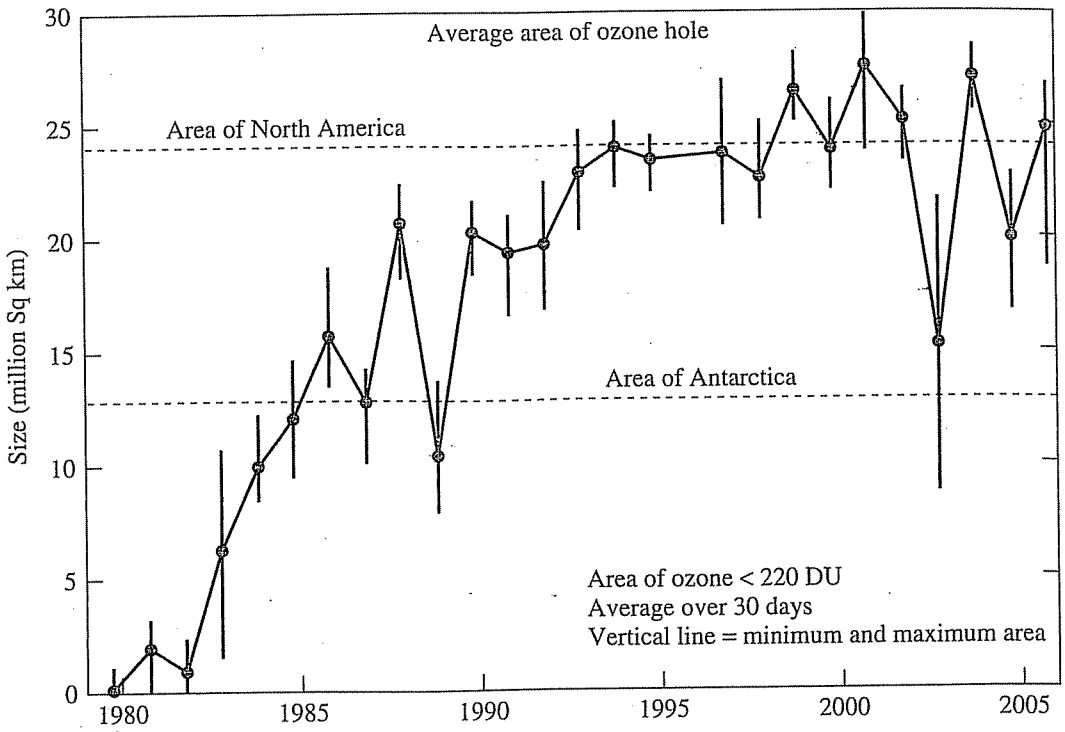

FIGURE 8.54 The average area of the ozone hole, defined as the region within which ozone is less than 220 DU, is about the size of North America.
(*Source:* NASA.)

enhancement could lead to stratospheric cooling, which would make an Arctic ozone hole more likely. Should an extensive ozone hole develop in the Northern Hemisphere, far more people would be exposed to elevated UV radiation.

Ozone Depletion Potential (ODPs)

The concept of Ozone Depletion Potentials (ODPs) for ozone-depleting substances (ODSs) is analogous to the Global Warming Potentials (GWPs) for greenhouse gases already described. In the case of ODPs, the reference gas is CFC-11 ($CFCl_3$). The ODP of a gas is defined as the change in total ozone per unit mass emission of the gas, relative to the change in total ozone per unit mass emission of CFC-11. Notice the definition of ODPs is independent of the length of time required for the depletion to take place, so, in that sense, they are somewhat different from time-dependent GWPs.

ODPs have become an integral part of the regulatory approach to controlling emissions of ozone-depleting substances. The Montreal Protocol on Substances that Deplete the Ozone Layer and its subsequent Amendments, which governs international production and use of halocarbons, and the U.S. Clean Air Act Amendments of 1990, which controls domestic uses, both dictate the phase-out of ozone-depleting substances based on their Ozone Depletion Potentials.

Table 8.10 lists ODPs for a number of CFCs, halons, and possible replacements. By definition, CFC-11 has an ODP of 1.0, which is the highest ODP of any of the CFCs. Halons-1211 and 1301 have much higher ODPs than CFC-11 due to the higher reactivity of bromine and the reduced effectiveness of deactivation traps

TABLE 8.10

Ozone Depletion Potentials (ODPs) and 100-Year Global Warming Potentials (GWPs) Measured Relative to CFC-11

Species	Chemical Formula	Ozone Depletion Potential Relative to CFC-11	Global Warming Potential Relative to CFC-11
CFC-11	$CFCl_3$	1.0	1.0
CFC-12	CF_2Cl_2	1.0	2.3
CFC-113	$C_2F_3Cl_3$	1.0	1.3
HCFC-22	CF_2HCl	0.05	0.4
HCFC-123	$C_2F_3HCl_2$	0.02	0.02
HCFC-124	C_2F_4HCl	0.02	0.12
HCFC-141b	$C_2FH_3Cl_2$	0.12	0.16
HFC-134a	$C_2H_2F_4$	0.0005	0.28
Halon-1211	CF_2ClBr	6	0.28
Halon-1301	CF_3Br	12	1.5
Methyl chloroform	CH_3CCl_3	0.1	0.03
Methyl bromide	CH_3Br	0.4	0.001

Source: WMO, *The Scientific Assessment of Ozone Depletion,* 2002.

compared with chlorine. Notice the replacement HCFCs have low ODPs, typically less than 0.1, which is a reflection of their short atmospheric lifetimes.

For comparison, 100-year GWPs relative to CFC-11 rather than the usual CO_2 reference molecule have been added to Table 8.10. These GWPs tell us that the HCFC and HFC replacements for CFCs are not only much better in terms of ozone depletion, but they also cause considerably less global warming. The halons, on the other hand, tend to be worse than CFCs in both categories.

Impacts of Increased Exposure to UV

The biological response to increased ultraviolet radiation is often represented by an *action spectrum.* The action spectrum provides a quantitative way to express the relative ability of various wavelengths to cause biological harm. For example, the action spectra for plant damage, DNA damage, and erythema (skin reddening) are shown in Figure 8.55*a*. All of these spectra show increasing damage as wavelength decreases, and they all show significant damage in the UV-B (280 to 320 nm) region. There are some differences, however. Plants, for example, show no damage from wavelengths above about 320 nm, but erythema damage occurs well into the UV-A (320 to 400 nm) portion of the solar spectrum. Sunscreens that block UV-B, but not UV-A, can give a false sense of security by allowing people to spend more time exposed to the sun without burning, but skin damage that may lead to skin cancer is occurring nonetheless.

By combining wavelength-dependent action spectra, such as are shown in Figure 8.55*a*, with ground-level solar irradiances, a biological weighted effectiveness of radiation is obtained. Figure 8.55*b* shows a representative action spectrum superimposed on two solar irradiance curves—one showing irradiance with an intact ozone layer (dotted line), and the other with an ozone layer that has been thinned somewhat (solid line). As the ozone column is depleted, the irradiance in those

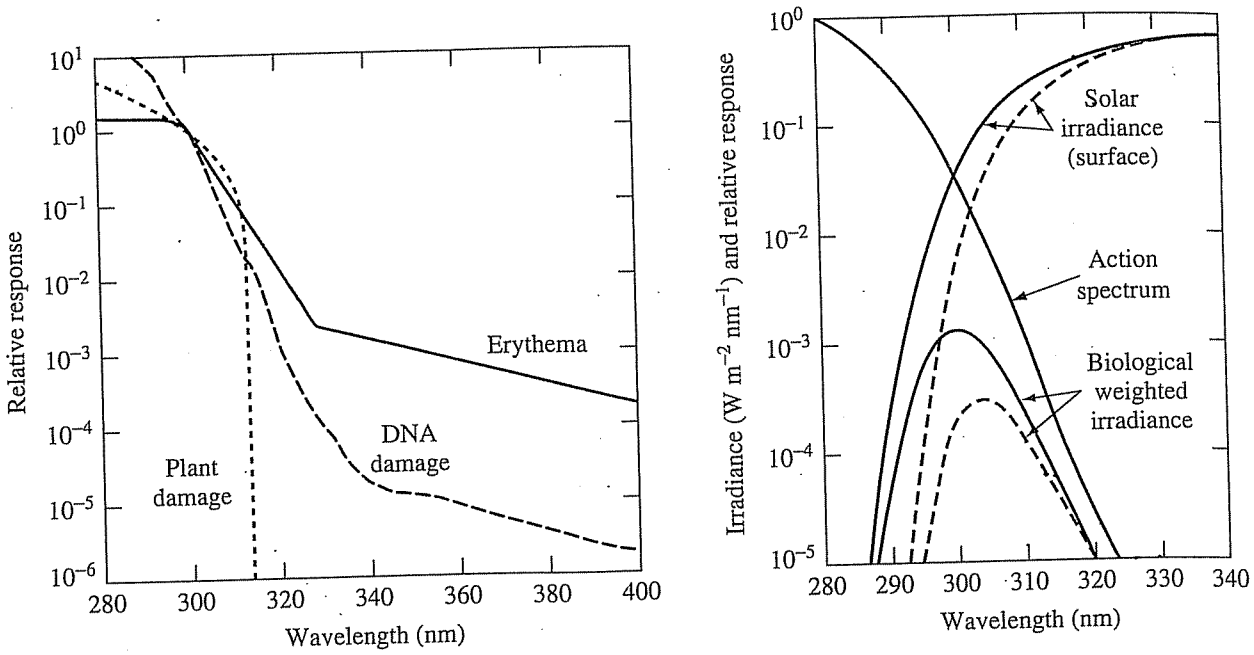

FIGURE 8.55 (*a*) Action spectra for damage to plants, DNA, and human skin; (*b*) by combining the action spectra with solar irradiance a biological weighted irradiance is obtained. The dotted lines represent irradiance under normal ozone conditions, while the solid lines correspond to a reduction in ozone.
(*Source:* Simon, 1993; Madronich, 1993.)

critical short UV-B wavelengths, where organisms are most sensitive, rises rapidly, as does the potential biological damage. The biologically weighted irradiance shows the critical wavelengths in terms of biological damage between about 290 and 310 nm (UV-B). Shorter wavelengths are effectively blocked by the remaining ozone layer, while longer wavelengths do little biological damage.

Most of our concern for increasing exposure to UV radiation has focused on the increased probability of developing skin cancer. Numerous studies have shown that skin cancer is readily induced in laboratory animals exposed to broad spectrum UV radiation, and the International Agency for Research on Cancer (1992) states unequivocally that "there is sufficient evidence in humans for the carcinogenicity of solar radiation. Solar radiation causes cutaneous malignant melanoma and non-melanocytic skin cancer." In fact, exposure to solar radiation is probably the main cause of all forms of skin cancer and an important, if not the main, cause of cancer of the lip (Armstrong, 1993).

Skin cancer is usually designated as being either the more common non-melanoma (basal cell or squamous cell carcinomas), or the much more life-threatening malignant melanoma. Epidemiological studies directly link skin cancer rates with exposure to UV-B. At lower latitudes, there is more surface-level UV-B, and skin cancer rates increase proportionately. Using such data, it has been estimated that a 1 percent increase in UV-B is estimated to cause a 0.5 percent increase in the incidence rate of melanoma and a 2.5 percent increase in nonmelanoma (Armstrong, 1993). Both types of skin cancer are more prevalent among people with fair complexion than among individuals who have more of the protective pigment, melanin.

Nonmelanoma is most likely to occur on areas of the skin habitually receiving greatest exposure to the sun, such as the head and neck. While it is rarely fatal, it

often causes disfigurement. Melanomas, on the other hand, are as common on intermittently exposed parts of the body, such as the trunk and legs, as they are on the head and neck. Melanomas seem to occur more frequently on individuals who have had severe and repeated sunburns in childhood. This observation has led to a hypothesis that melanoma is less related to the accumulated dose of radiation, as seems to be the case for nonmelanoma, than it is to the pattern of exposure.

The incidence rate of melanoma among fair skinned individuals in the United States is increasing at 2 to 3 percent annually, which is faster than any other form of cancer. In 1935, the lifetime risk of an American developing melanoma was 1 in 1,500 individuals, while in 2002 the risk was 1 in 68. Approximately 54,000 melanomas are diagnosed each year, and 7,600 die of the disease. While some are tempted to relate that increase to the thinning of the ozone layer, it is much more likely to be the result of lifestyle changes rather than increased surface-level UV irradiation. More people are simply spending more time outdoors in the sun than in the past. Moreover, the decrease in stratospheric ozone is a relatively recent phenomenon, and evidence suggests that skin cancer may have a long latency period. There very well may be a 20-year lag time between changes in solar irradiance and measurable increases in skin cancer caused by that exposure.

To help alert the public to the dangers of UV exposure, various versions of a simple index have been created. A UV-index is a nondimensional, single number, in the range of 0 to 12, that represents an erythemal-weighted irradiance expected at solar noon (when the sun is at its highest) for the following day. The UV-index is now a routine part of Web and newspaper weather forecasts. To make the index more appealing and understandable for the public, it is linked to descriptive words ranging from "Low" to "Extreme," and it also provides an estimate of the length of time required for a fair-skinned person to get sunburned. The World Health Organization index is shown in Table 8.11.

Other human health problems associated with UV exposure include ocular damage (cataracts and retinal degeneration) and immune system suppression. The effects of increasing UV-B radiation would not be felt by humans alone, of course. There is considerable evidence that UV-B reduces photosynthesis and other plant processes in terrestrial and aquatic plants. UV-B radiation is known to penetrate to ecologically significant depths in the oceans, and besides impairing photosynthesis, it threatens marine organisms during their critical developmental stages. For example, amphibian eggs have little protection when exposed to UV-B irradiation, and the worldwide decline in frogs and toads, especially at high altitudes where solar exposure is greatest, may be in part caused by our thinning ozone layer.

TABLE 8.11

WHO Exposure Levels and Sunburn Warnings

UV Index	Category Descriptor	Sunburn Time
1–2	Low	More than 1 hour
3–5	Moderate	45 minutes
6–7	High	30 minutes
8–10	Very High	15 minutes
11+	Extreme	Less than 10 minutes

Political Response to the Ozone Depletion Problem

The political response to warnings of ozone depletion by the scientific community has been unusually effective and timely. When CFCs were first created in the 1930s they were hailed as wonder chemicals. They replaced toxic, explosive, and unstable refrigerants and made possible the refrigeration and air conditioning luxuries that we now take for granted.

A British scientist, James E. Lovelock (later famous for the "Gaia"), began experimenting with CFCs in the 1970s and concluded in 1973 that essentially all of the CFCs ever produced were still in the atmosphere. The first hint of potential problems came with the publication of Molina and Rowland's paper in 1974, which warned of the danger to the stratospheric ozone layer that CFCs presented. The EPA responded in a remarkably short period of time and banned nonessential spray-can uses of CFCs by 1979. A few countries followed the U.S. lead, including Canada and some of the Scandinavian countries, but most continued to manufacture and use them without concern for the consequences. It wasn't until the discovery of the ozone hole over Antarctica in 1985 that the rest of the world awakened to the lurking danger. At that time, worldwide CFC use as an aerosol propellant was the largest single source of CFC emissions.

In 1987 an international meeting convened in Montreal that led to the signing of the *Montreal Protocol on Substances that Deplete the Ozone Layer*. That Protocol called for a 50 percent reduction in use of CFCs by 1999. It was soon realized, however, that the called-for reductions were inadequate, and in 1990, 93 nations convened in London and created a new timetable calling for a complete phase-out of CFCs, most halons, and carbon tetrachloride by the year 2000. The plight of the developing countries was recognized and their use of CFCs was extended to 2010. A fund was established to help pay for technology transfer to enable the less-developed countries to take advantage of proposed replacement chemicals.

The next year, 1991, Mt. Pinatubo erupted, and the ozone hole grew to record proportions, which led to the London Amendments to the Protocol in 1992. The phase-out of CFCs was moved up to 1996.

Meanwhile, in the United States, Title VI of the Clean Air Act Amendments of 1990 brought us into compliance with the London Amendment. Major provisions include the following:

- Two categories of ozone-depleting substances (ODS) were created: Class I chemicals are those with high ozone depletion potentials, which includes CFCs, halons, and carbon tetrachloride, and Class II substances have lower ODPs and include the HCFCs. Production of Class I chemicals was scheduled to cease by 2000, while Class II chemicals are subject to an accelerated phase-out schedule that will eliminate all production and use by 2030. Exceptions for necessary medical, aviation, safety and national security purposes, and for export to developing countries are allowed.
- Motor vehicle air conditioners received special attention since they had been the largest single source of CFCs. CFC recycling equipment for air conditioner servicing is required, and only certified repair persons are allowed to do the work. CFCs must be removed from car air conditioners before they are crushed for disposal.

- Nonessential products that use ozone-depleting substances such as noise horns, "silly string," and some commercial photographic equipment, are banned.
- Warning labels are required for products that contain ODS such as refrigerators and foam insulation.
- Modifications to the Montreal Protocol that accelerate the phasing out of ODS must be adhered to.

Two years later, in 1992, the Copenhagen Amendments to the Montreal Protocol called for participating nations to move the ban of many ODSs to 1996. The EPA responded in 1993 with an accelerated phase-out schedule. Production and imports of halons ceased in 1994, and CFCs, methyl chloroform (1,1,1-trichloroethane), and carbon tetrachloride ceased in 1996. Most HCFCs were eliminated by 2003, but some will still be allowed until 2030.

Has this flurry of regulatory activity been effective? Stratospheric ozone depletion is one of those problems that cannot be reversed in a short period of time. Most of the CFCs ever produced are still drifting around in the atmosphere and they will be with us for decades into the future. The production cuts dictated by the Montreal Protocol and subsequent Amendments have already stopped the steady, historical climb in CFC atmospheric concentration. Figure 8.56 sums up the good news. CFC production has stopped, though HCFCs will still be produced until 2030; the major ozone-destroying chlorine and bromine concentrations in the stratosphere have begun to decline; and the overall global stratospheric ozone concentration is beginning to recover. Not only have countless lives been saved, but the Montreal Protocol has provided a model for effective international cooperation on a major global environmental problem.

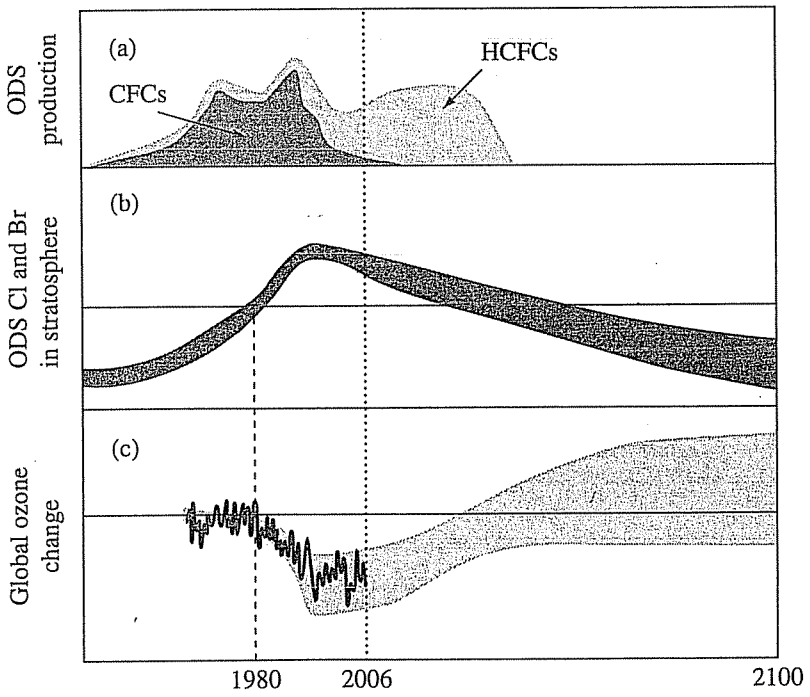

FIGURE 8.56 A global environmental success story. (a) Production of CFCs has ended, and HCFCs are scheduled to be phased out; (b) stratospheric chlorine and bromine are beginning to decline; (c) global ozone shows signs of recovery.
(*Source:* WHO/UNEP, *Scientific Assessment of Ozone Depletion,* 2006.)

PROBLEMS

8.1 Suppose an ocean sediment sample shows $(^{18}O/^{16}O) = 0.0020150$. Using the VSMOW for seawater, what is the value of $\delta^{18}O$? Is this a sign of more or less glaciation at the time the sediment was deposited?

8.2 The following data are from a Vostok ice core. Plot the data, and from the slope, estimate the temperature change in δD per °C.

Depth (m)	Years Before Present	Delta D ($^0/_{00}$)	Temperature (°C)
280	12087	−448.5	−3.09
327	14904	−458.1	−4.68
346	16201	−468.5	−6.34
355	16889	−480.7	−8.33
365	17706	−478.0	−7.84

8.3 Suppose an ice core measurement taken from the last glacial period resulted in the isotope ratio $(^2H/^1H) = 8.100 \times 10^{-5}$.

(a) Find the corresponding $\delta D(^0/_{00})$ using the 0.00015575 VSMOW standard for deuterium.

(b) If an interglacial sample had $\delta D(^0/_{00}) = -435$ per mil, how much warmer was the interglacial period assuming a 6 per mil change in $\delta D(^0/_{00})$ corresponds to a 1°C temperature change?

8.4 A relationship between the mean annual surface temperature of Greenland and the value of $\delta^{18}O$ of the snow pack on the Greenland ice sheet is given by

$$T(°C) = 1.5\delta^{18}O(^0/_{00}) + 20.4$$

An ice core sample dating back to the last glacation has a value of $\delta^{18}O$ equal to −35. What would the estimated surface temperature have been at that time?

8.5 Use the following ice core data to derive a relationship between T(°C) and δD similar to the one shown in Problem 8.4 for ^{18}O.

Depth (m)	Years Before Present	Delta D ($^0/_{00}$)	Temperature (°C)
0	0	−438.0	0
12	234	−449.1	−1.84
20	420	−435.9	0.35
47	1247	−446.9	−1.48
68	2049	−440.3	−0.38
143	5397	−435.0	0.5

8.6 Suppose the Earth is really flat (Figure P8.6). Imagine an Earth that is shaped like a penny, with one side that faces the sun at all times. Also suppose that this flat Earth is the same temperature everywhere (including the side that faces away from the sun). Neglect any

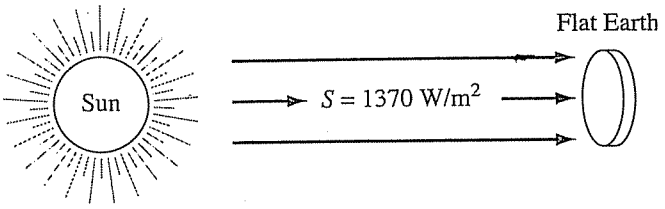

FIGURE P8.6

radiation losses off of the rim of the Earth, and assume there is no albedo or greenhouse effect. Treating it as a perfect blackbody, estimate the temperature of this new, flat Earth.

8.7 The solar flux S striking a planet will be inversely proportional to the square of the distance from the planet to the sun. That is, $S = k/d^2$, where k is some constant and d is the distance. Using data from Table 8.2 to find k,

(a) Estimate the solar constant for the planet Mercury.

(b) If Mercury is 58×10^6 km from the sun and has an albedo of 0.06, find its effective temperature.

(c) At what wavelength would the radiation spectrum from Mercury reach its peak?

8.8 The solar flux S arriving at the outer edge of the atmosphere varies by ± 3.3 percent as the Earth moves in its orbit (reaching its greatest value in early January). By how many degrees would the effective temperature of the Earth vary as a result?

8.9 In the article "The Climatic Effects of Nuclear War" (*Scientific American*, August 1984), the authors calculate a global energy balance corresponding to the first few months following a 5,000-megaton nuclear exchange. The resulting smoke and dust in the atmosphere absorb 75 percent of the incoming sunlight (257 W/m^2), while the albedo is reduced to 20 percent. Convective and evaporative heating of the atmosphere from the Earth's surface is negligible, as is the energy reflected from the Earth's surface. The Earth's surface radiates 240 W/m^2, all of which is absorbed by the atmosphere. Assuming that the Earth can be modeled as a blackbody emitter as shown in Figure P8.9, find the following (equilibrium) quantities:

(a) The temperature of the surface of the Earth (this is the infamous "nuclear winter")

(b) X, the rate at which radiation is emitted from the atmosphere to space

(c) Y, the rate of absorption of short-wavelength solar radiation at the Earth's surface

(d) Z, the rate at which the atmosphere radiates energy to the Earth's surface

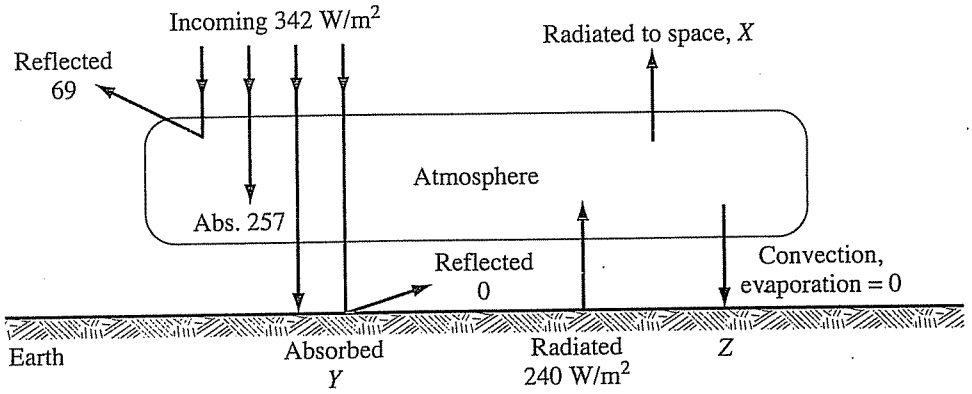

FIGURE P8.9

8.10 Consider the two-layer atmospheric model shown in Figure P8.10. An advantage of this model is it allows us to model radiation so that each layer radiates the same amount off its top and bottom. Find the unknown quantities W, X, Y, and Z to make this model balance. What values of T_1 and T_2 would radiate W and Z?

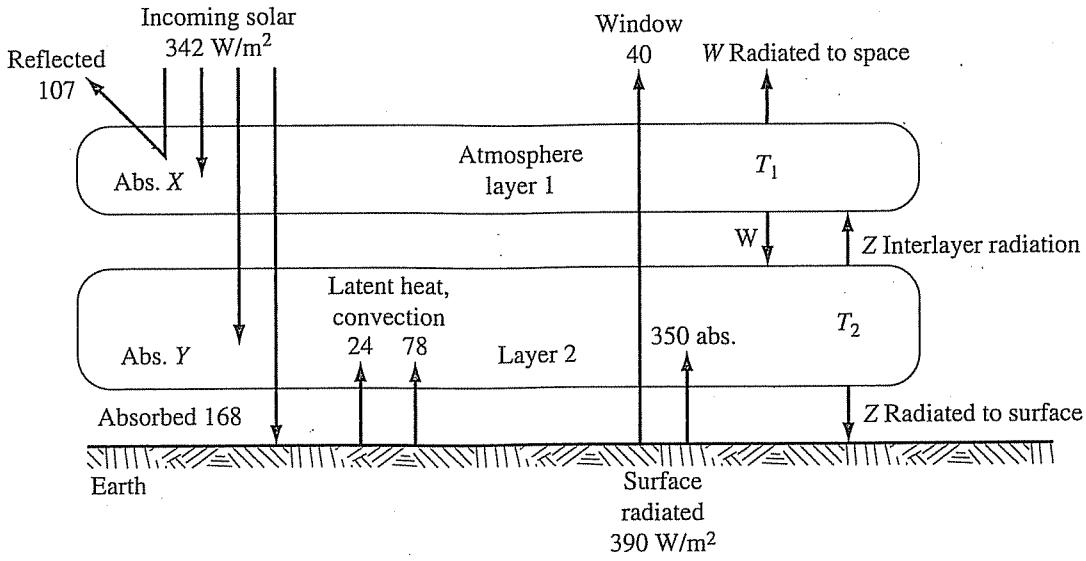

FIGURE P8.10

8.11 In Figure 8.12, the average rate at which energy is used to evaporate water is given as 78 W/m^2. Using 2,465 kJ/kg as the latent heat of vaporization of water, along with the surface area of the Earth, which is about 5.1×10^{14} m^2, estimate the total world annual precipitation in m^3/yr (which is equal to the total water evaporated). Averaged over the globe, what is the average annual precipitation in meters of water?

8.12 Suppose a greenhouse effect enhancement raises the surface temperature of the Earth to 291 K, melting enough snow and ice to reduce the albedo to the point where only 100 W/m^2 are reflected (see Figure P8.12). The atmospheric window is closed somewhat so that only 30 W/m^2 now pass directly from the Earth's surface to space. If the latent and sensible heat transfer to the atmosphere do not change, and if incoming solar energy absorbed by the atmosphere does not change, find the solar radiation absorbed at the

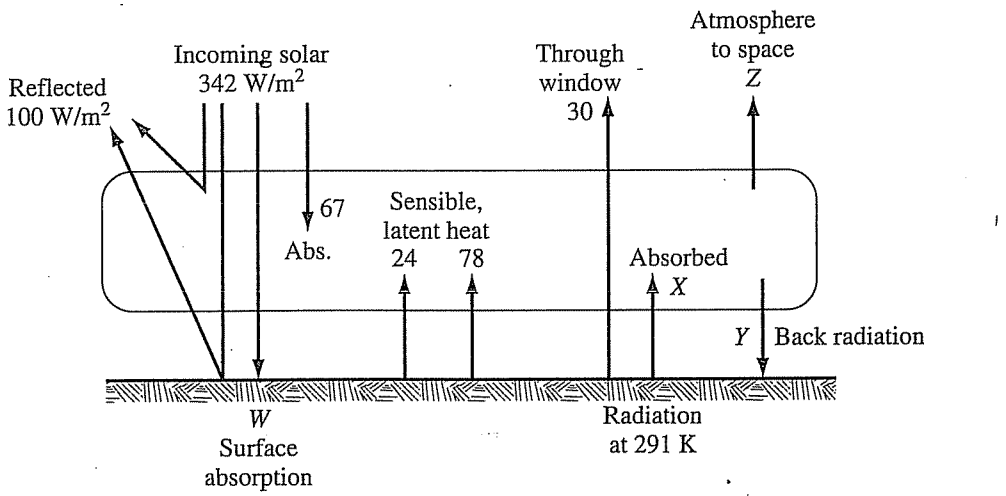

FIGURE P8.12

surface W, the surface radiation X absorbed by the atmosphere, the back radiation from atmosphere to the surface Y, and the outgoing radiation from the atmosphere Z so that energy balance is maintained in each of the three regions (space, atmosphere, surface).

8.13 What would the atmospheric concentration of CO_2 be 50 years from now if carbon emissions rise linearly from 10 GtC/yr to 16 GtC/yr over that period of time. Assume the initial CO_2 concentration is 380 ppm, and use a 40 percent airborne fraction.

8.14 Suppose atmospheric CO_2 is growing at 2 ppm/yr, fossil fuel and cement emissions are 9 GtC/yr, and the airborne fraction is 38 percent. If the only other carbon emissions are associated with land use changes, estimate their net carbon emission rate.

8.15 The United States derives about 40 percent of its energy from oil, 23 percent from coal, and 23 percent from natural gas, with the remaining 14 percent from essentially carbon-free sources.

(a) Using LHV values for carbon intensity for each fuel, estimate the overall carbon intensity.

(b) Suppose all of that coal is replaced with carbon-free nuclear and renewable energy systems; what would be the new carbon intensity?

(c) Suppose that transition takes 100 years. Modeled as an exponential change, what rate of growth in carbon intensity does that correspond to?

8.16 Using estimates of the total resource base of coal, petroleum, and natural gas given in Table 8.4, along with LHV carbon intensities given in Table 8.3, and with an assumed airborne fraction of 50 percent, calculate the total increase in atmospheric CO_2 that would be caused by burning all of the

(a) Natural gas

(b) Petroleum

(c) Coal with 50 percent of the CO_2 captured and stored

(d) Burning all three as stated previously, what would be the equilibrium global temperature increase with a climate sensitivity factor $\Delta T_{2X} = 2.8°C$ and a current CO_2 concentration of 380 ppm?

8.17 Suppose that in 100 years the world is virtually out of natural deposits of oil and gas and energy demand is double the current rate of 330 EJ/yr. At that time, imagine that 28 percent of world energy comes from coal, 60 percent is synthetic gas and oil from coal with a LHV carbon intensity of 44 gC/MJ, and the remainder is derived from noncarbon-emitting sources. Using LHV values of carbon intensity,

(a) What would be the carbon emission rate then (Gt/yr)?

(b) If carbon emissions grow exponentially from the current rate of 6.0 GtC/yr to the rate found in part a, what rate of growth r would have prevailed during that 100 years?

(c) If the airborne fraction is 50 percent, how much of the carbon emitted in the next 100 years would remain in the atmosphere?

(d) What would be the atmospheric concentration of CO_2 in 100 years if there is no net contribution from biomass (and there are 750 Gt of carbon in the atmosphere now)?

(e) If the equilibrium temperature increase for a doubling of CO_2 is 3°C, what would be the equilibrium temperature increase in 100 years if the initial concentration is 356 ppm?

8.18 Suppose in 100 years energy consumption is still 330 EJ/yr, but coal supplies only 20 percent of total demand, natural gas supplies 30 percent, and oil 10 percent. The remaining

40 percent of demand is met by noncarbon-emitting sources such as nuclear and solar energy. Using this conservation scenario, repeat parts a through e of Problem 8.17.

8.19 One reason for sometimes using HHVs rather than LHVs is related to the strange efficiencies that may emerge when a conversion device actually takes advantage of the latent heat normally lost in flue gases. Suppose a methane-fired condensing furnace has an HHV efficiency of 95 percent. What would its LHV efficiency be?

8.20 For each of the following fuels, find the carbon intensity based on the higher heating values (HHV) given:

(a) Ethane, C_2H_6, HHV = 1,542 kJ/mol

(b) Propane, C_3H_8, HHV = 2,220 kJ/mol

(c) *n*-Butane, C_4H_{10}, HHV = 2,878 kJ/mol

8.21 Consider the following four ways to heat a house. The first uses a new high-efficiency pulse-combustion gas furnace; the second uses a conventional gas furnace; the third uses an electric heat pump that delivers 3 units of energy to the house for each unit of electrical energy that it consumes (the other 2 units are heat taken from the ambient air); and the fourth uses conventional electric heating. Using HHV values of carbon intensity (since these efficiencies are based on American definitions) and power plants fueled with coal, compute the carbon emissions per unit of heat delivered to the house (gC/MJ).

Option	Description	Furnace Efficiency (%)	Power Plant Efficiency (%)
1	Pulse-gas	95	—
2	Conventional gas	70	—
3	Heat pump	300	35
4	Electric	100	35

8.22 Supplement Example 8.8 with a water heater that burns propane (C_3H_8) with 85 percent efficiency.

(a) Propane releases 2,200 kJ of energy per g-mol; find its carbon intensity (gC/MJ).

(b) Find the ratio of carbon released to energy that actually heats the water (gC/MJ).

(c) What percentage of carbon emissions are saved using propane compared with electric heating from a natural-gas-fired power plant as computed in Example 8.8?

8.23 Disaggregated growth rates for three scenarios are given in the following table:

	Population (%/yr)	GDP/person (%/yr)	Energy/GDP (%/yr)	C/Energy (%/yr)	Airborne Fraction	Sensitivity ΔT_{2X}(°C)
(A)	1.0	0.3	−2.0	−0.7	0.4	3
(B)	1.5	1.5	−0.2	0.4	0.5	2
(C)	1.4	1.0	−1.0	−0.2	0.5	3

For each scenario,

(a) Predict CO_2-induced global equilibrium temperature increase in 70 years, if the initial CO_2 concentration is 356 ppm, the initial emission rate is 6.0 Gt/Cyr, and the initial atmospheric carbon content is 750 GtC.

(b) If those growth rates continue, in what year would CO_2 concentrations be equal to double the initial 356 ppm?

8.24 The expanded Kaya analysis (8.28) applied to SRES scenario A2 averaged from 1990 to 2100 has the following energy-component growth rates:

Population growth rate $dP/dt = 0.8\%$
Per capita GDP growth rate $d(\text{GDP/P})/dt = 1.3\%$
Final Energy per GDP growth rate $= d(\text{FE/GDP})/dt = -0.7\%$
Primary Energy to Final Energy growth rate $d(\text{PE/FE})/dt = 0.1\%$
Carbon per unit of Primary Energy growth rate $d(\text{TC/PE})/dt = -0.2\%$
Carbon Sequestration growth rate $d(\text{C/TC})/dt = 0.0\%$

With 1990 energy-related carbon emissions equal to 6.0 GtC/yr and growing at the above rates, and land-use and industrial emissions a constant 2.5 GtC/yr:

(a) What would the carbon emission rate be in 2100?

(b) What total carbon would have been emitted?

(c) With an Airborne Fraction of 0.5, what would be the increase in CO_2 concentration due to these energy-related carbon emissions?

(d) With 360 ppm CO_2 in 1990, what would be the concentration in 2100?

(e) With $\Delta T_{2X} = 2.8°C$, estimate the increase in global equilibrium temperature in 2100 relative to 1990.

8.25 Indicate whether the following halocarbons are CFCs, HCFCs, HFCs, or halons, and give their designation numbers:

(a) C_3HF_7

(b) $C_2FH_3Cl_2$

(c) $C_2F_4Cl_2$

(d) CF_3Br

8.26 Write chemical formulas for the following:

(a) HCFC–225

(b) HFC–32

(c) H–1301

(d) CFC–114

8.27 What feedback climate sensitivity λ and factor g would correspond to the following values of ΔT_{2X}? For each, estimate the change in ΔT_{2X} that would result if the feedback factor g increases by 0.1.

(a) $\Delta T_{2X} = 2.5°C$

(b) $\Delta T_{2X} = 3.5°C$

8.28 Figure 8.39 shows two probability density functions for the climate sensitivity factor ΔT_{2X} labeled WR and AS.

(a) Estimate the AS probability that ΔT_{2X} is less than 2.5°C.

(b) Estimate the WR probability that ΔT_{2X} is greater than 3°C.

(c) Estimate the AS probability that ΔT_{2X} is between 3°C and 4°C.

(d) Estimate the WR probability that ΔT_{2X} is between 3°C and 4°C.

8.29 The radiative forcing as a function of concentration for N_2O is sometimes modeled as follows, where C and C_0 are final and initial ppb concentrations:

$$\Delta F = k_2(\sqrt{C} - \sqrt{C_0})$$

Assuming it has been in that region since preindustrial times when the concentration was 275 ppb, find an appropriate k_2 if the current concentration is 311 ppb and the forcing is estimated to be 0.14 W/m^2. Estimate the added radiative forcing in 2100 if it reaches a concentration of 417 ppb.

8.30 The following is an estimate for radiative forcing caused by the principal greenhouse gases:

$$\Delta F = 6.3 \ln\frac{[(CO_2)]}{[(CO_2)_0]} + 0.031(\sqrt{CH_4)} - \sqrt{(CH_4)_0}) + 0.133(\sqrt{(N_2O)} - \sqrt{(N_2O)_0}) + 0.22[(CFC{-}11) - (CFC{-}11)_0] + 0.28[(CFC{-}12) - (CFC{-}12)_0]$$

where concentrations are expressed in ppb and ΔF is in W/m^2. Using the following data for atmospheric concentrations:

Year	CO_2 (ppm)	CH_4 (ppb)	N_2O (ppb)	CFC–11 (ppb)	CFC–12(ppb)
1850	278	700	275	0	0
1992	356	1714	311	0.268	0.503
2100	710	3616	417	0.040	0.207

(a) What would be the combined radiative forcing caused by these gases from 1850 to 1992?

(b) What would be the forcing from 1992 to 2100?

(c) What would be the forcing from 1850 to 2100?

8.31 What would be the equilibrium temperature change from 1850 to 2100 for the combination of greenhouse gases described in Problem 8.30 if the climate sensitivity parameter λ is 0.57°C per W/m^2?

8.32 For most greenhouse gases, injection of 1 kg into the atmosphere decays exponentially with time (but not CO_2), so their GWP equation (8.43) can be simplified to the following:

$$GWP_g = \frac{\int_0^T F_g \cdot R_g(t)dt}{\int_0^T F_{CO_2} \cdot R_{CO_2}(t)dt} = \left(\frac{F_g}{F_{CO_2}}\right) \cdot \frac{\int_0^T e^{-t/\tau}dt}{\int_0^T R_{CO_2}(t)dt}$$

where τ is their residence time (Table 8.7). For CO_2, the integral for 20-yr, 100-yr, and 500-yr GWPs has been estimated to be roughly the following

$$\int_0^{20} R_{CO_2}(t)\,dt \approx 13.2 \text{ yrs}; \quad \int_0^{100} R_{CO_2}(t)\,dt \approx 43.1 \text{ yrs}; \quad \int_0^{500} R_{CO_2}(t)\,dt \approx 138 \text{ yrs}$$

For HFC-134a, $(F_g/F_{CO_2}) = 4{,}129$ and $\tau = 14$ yrs. Compute its GWP for the following time horizons and compare your results with Table 8.7.

(a) 20 years

(b) 100 years

(c) 500 years

8.33 Using the procedure described in Problem 8.32, compute the global warming potential for a greenhouse gas having an atmospheric lifetime $\tau = 42$ years and a relative forcing per unit mass that is 1,630 times that of CO_2. Do this for a time period of:

(a) 20 years

(b) 100 years

(c) 500 years

8.34 The IS92a emission scenario suggests anthropogenic emissions in 2025 equal to the following: $44{,}700 \times 10^9$ kg CO_2; 320×10^9 kg CH_4; and 22×10^9 kg N_2O. Weighting these by their global warming potentials, what fraction of the total impact of that year's emissions of these three gases would be caused by each gas over the following time periods?

(a) 20 years

(b) 100 years

(c) 500 years

8.35 In 2006, the United States emitted 6,000 million metric tons (Mt) of CO_2, 26.6 $MtCH_4$, and 1.2 MtN_2O. Using 100-year global warming potentials, what is the equivalent CO_2 emission rate of the total for these three gases, in GtC-eq/yr.

8.36 Direct greenhouse gas radiative forcing in the mid-1990s is estimated to be about 2.45 W/m^2. If realized temperature is 75 percent of equilibrium temperature, what negative forcing by aerosols, and so on, would be needed to match the 0.6°C realized global temperature increase actually observed? Assume that an appropriate climate sensitivity factor λ is 0.57.

8.37 Repeat Example 8.12, but this time use a 100-yr instead of the 20-yr GWP for methane leakage.

8.38 Based on a 1990 world fossil-fuel carbon emission rate of 6.0 Gt/yr and total fossil fuel carbon ever emitted equivalent to the consumption of 200,000 EJ of coal (LHV) for each of the following values of maximum emission rate, plot a graph of carbon emissions vs. time using a Gaussian emission function described in Chapter 3 (Equations 3.17 to 3.20). In what year would maximum emissions occur?

(a) Maximum emission rate of 22 GtC/yr

(b) Maximum emission rate of 34 GtC/yr

(c) Maximum emission rate of 58 GtC/yr

8.39 Many economists favor a carbon tax as a way to discourage CO_2 emissions. Suppose such a tax were to be set at $20 per metric ton of carbon emissions as (CO_2). Consider a small, 50-MW, 35 percent-efficient coal-fired power plant. Using a carbon intensity for coal of 24 gC/MJ,

(a) What would the annual carbon tax be for this power plant assuming capacity factor of 100%?

(b) Suppose a tree plantation sequesters (removes from the atmosphere and stores in biomass) on the order of 5,000 kg of carbon per year per acre over the 40 years that the trees are growing (after which time the forest is mature, and no further accumulation of carbon occurs). What area of forest would have to be planted to "offset" the power plant's emissions over the next 40 years (roughly the lifetime of the power plant)?

(c) How much could the owners of the plant pay for the forestry project ($/acre per year) and still have it be cheaper than paying the $20/metric ton carbon tax?

8.40 Suppose a landfill leaks 10 tonnes (1 tonne = 1 metric ton = 1000 kg) of methane CH_4 into the atmosphere each year.

(a) Using methane's 20-year GWP, what would the warming (radiative forcing) be equivalent to in terms of tonne/yr of CO_2 emissions?

(b) Suppose a soil-vapor extraction system is installed at the landfill to suck up the methane before it leaks into the atmosphere. If that methane is burned, the methane is converted to CO_2. What would be the CO_2 emissions per year now?

(c) What is the equivalent CO_2 savings by burning the methane? How many tonnes per year of C emissions (as CO_2) would be saved?

(d) If a carbon tax of \$20/tonne of C (as CO_2) is enacted, how much tax could be saved per year by burning the methane instead of letting it leak out of the landfill?

(e) A carbon tax of \$20/tonne of C is the same as a tax of \$5.45 per tonne of CO_2 (carbon is 12/44ths of the mass of CO_2). Using the tons of CO_2 equivalents found in a, how much tax could be saved per year if the methane is burned instead of letting it leak out of the landfill?

8.41 Gasoline is approximately C_7H_{15}, and 1 gallon of it weighs about 6.15 pounds. Assume that all of the carbon in gasoline is emitted as CO_2 when it is burned.

(a) Suppose an old car that only gets 12 miles per gallon (mpg) will be driven 40,000 more miles before it ends up in the junk yard. How much carbon will it emit during that time?

(b) If the car weighs 4,000 pounds, and it is driven 10,000 miles per year, what is the ratio of the weight of carbon emitted per year to the weight of the car?

(c) Suppose there is a carbon tax of \$15 per ton of carbon (\$4.08 per ton of CO_2). What would the carbon tax be on 1 gallon of gasoline?

(d) How much would carbon emissions be reduced over those 40,000 miles if that old car is replaced with a new one that gets 40 mpg?

(e) If an electric utility is trying to reduce its carbon tax by offering incentives to get older cars off the road, how much should the utility be willing to pay to encourage the owner of the old clunker to trade it in on a 40-mpg car?

8.42 Consider the potential carbon emissions from a gasoline-powered car compared with the carbon emissions to make the electricity for an electric car.

(a) Suppose the conventional car gets 40 miles per gallon (mpg). What are the carbon emissions (gC/mi) assuming that gasoline contains 5.22 pounds of carbon per gallon?

(b) An efficient combined-cycle, natural-gas-fired power plant needs about 8,000 kJ of heat to generate 1 kWh of electricity. At 13.8 gC/MJ for natural gas, what would be the carbon emissions (gC/mi) for an electric vehicle that gets 5 miles/kWh?

(c) Suppose an older, 30 percent-efficient coal-fired power plant generates the electricity that powers that electric car. At a carbon intensity of 24 gC/MJ for coal, what would the carbon emissions be (gC/mi) for that 5 mi/kWh electric car?

8.43 The photon energy required to cause the following reaction to occur is 306 kJ/mol. What is the maximum wavelength that the photon can have?

$$NO_2 + h\nu \rightarrow NO + O$$

8.44 Photodissociation of oxygen requires 495 kJ/mol. What maximum wavelength can the photon have to drive this reaction?

$$O_2 + h\nu \rightarrow O + O$$

REFERENCES

Armstrong, B. K., 1993, Implications of increased solar UVB for cancer incidence, *The Role of the Stratosphere in Global Change,* M. Chanin (ed.), Springer-Verlag, Berlin.

Arrhenius, S., 1896, On the influence of carbonic acid in the air upon the temperature of the ground, *Philosophical Magazine and Journal of Science,* S. 5, 41(251), 237–276.

Andronova, N. G., and M. E. Schlesinger, 2001, Objective estimation of the probability density function for climate sensitivity, *J. of Geophysical Research D: Atmospheres,* 106(D19), 22605–22611.

Baird, C., 1995, *Environmental Chemistry,* W. H. Freeman, New York.

Broecker, W. S., and G. H. Denton, 1990, What drives glacial cycles?, *Scientific American,* January, 49–56.

Caldeira, K., and M. E. Wickett, 2003, Anthropogenic carbon and ocean pH, *Nature,* 435, 365, September 25.

Dansgaard, W., and H. Oeschger, 1989, Past environmental long-term records from the Arctic, *The Environmental Record in Glaciers and Ice Sheets,* H. Oeschger and C. C. Langway (eds.), John Wiley & Sons, New York.

Edmonds, J., and J. Reilly, 1983, Global energy production and use to the year 2050, *Energy,* 8, 419.

Ehrlich, P., and J. Holdren, 1971, Impact of population growth, *Science,* 171, 1212–1217.

Energy Information Administration (EIA), 2006, *Emissions of Greenhouse Gases in the United States 2005,* U.S. Department of Energy, Washington, DC.

Frederick, J. E., 1986, The ultraviolet radiation environment of the biosphere, *Effects of Changes in Stratospheric Ozone and Global Climate,* Vol. 1, USEPA and UNEP, Washington, DC.

Henderson-Sellers, A., and K. McGuffie, 1987, *A Climate Modelling Primer,* John Wiley & Sons, New York.

Hansen, J. E., R. Ruedy, M. Sato, M. Imhoff, W. Lawrence, D. Easterling, T. Peterson, and T. Karl, 2001, A closer look at United States and global surface temperature change, *J. Geophys. Res.,* 106, 23947–23963.

Hansen, J., 2004, The role of soot in global climate change, *Black Carbon Emissions and Climate Change: A Technical Workshop,* Oct 13–15, National Renewable Energy Laboratory, San Diego, CA.

Houghton, R. A., 2003, Revised estimates of the annual net flux of carbon to the atmosphere from changes in land use and land management 1850–2000, *Tellus,* 55B, 378–390.

Hummel, H., 2006, *Interpreting Energy and Emission Scenarios: Methods for Understanding and Communicating Policy Insights,* Ph.D. Thesis, Stanford University, Stanford, CA.

Houweling, S., T. Kaminski, F. Dentener, and J. Lelieveld, 2006, Inverse modeling of methane sources and sinks using the adjoint of a global transport model, *Nature,* 439, 187–191, January, 12.

Imbrie, J., J. D. Hays, D. G. Martinson, A. McIntyre, A. C. Mix, J. J. Morley, N. G. Pisias, W. I. Pell, and N. J. Shackleton, 1984, Orbital theory of the Pleistocene climate: Support from a revised chronology of the marine $\delta^{18}O$ record, in *Milankovitch and Climate,* Part I, A. Berger, J. Imbrie, J. Hays, G. Kukla, and B. Saltzman (eds.), D. Reidel Publishing Co., Dordrecht. pp 269–305.

Intergovernmental Panel on Climate Change (IPCC), 1990, *Climate Change: The IPCC Scientific Assessment,* Cambridge University Press, Cambridge, UK.

Intergovernmental Panel on Climate Change (IPCC), 1992, *Climate Change 1992,* Cambridge University Press, Cambridge, UK.

Intergovernmental Panel on Climate Change, 1995, *Climate Change 1994: Radiative Forcing of Climate Change,* Cambridge University Press, Cambridge, UK.

Intergovernmental Panel on Climate Change, 1996, *Climate Change 1995: The Science of Climate Change,* Cambridge University Press, Cambridge, UK.

Intergovernmental Panel on Climate Change (IPCC), 2000, *IPCC Special Report: Emissions Scenarios,* Cambridge University Press, Cambridge, UK.

Intergovernmental Panel on Climate Change (IPCC), 2007, *Climate Change 2007: The Physical Science Basis,* Cambridge University Press, Cambridge, UK.

International Agency for Research on Cancer, 1992, *Solar and Ultraviolet Radiation,* IARC monographs on the evaluation of carcinogenic risks to humans, Vol. 55, IARC, Lyon.

Jouzel, J., N. I. Barkov, J. M. Barnola, M. Bender, J. Chappellaz, C. Genthon, V. M. Kotlyakov, V. Lipenkov, C. Lorius, J. R. Petit, D. Raynaud, G. Raisbeck, C. Ritz, T. Sowers, M. Stievenard, F. Yiou, and P. Yiou, 1993, Extending the Vostok ice-core record of paleoclimate to the penultimate glacial period, *Nature,* 36, 407–412.

Kiehl, J. T., and K. E. Trenberth, 1996, Earth's annual global mean energy budget, *Bulletin of the American Meteorological Society* (submitted).

Kaya, Y., 1990, Impact of carbon dioxide emission control on GNP growth: Interpretation of proposed scenarios, *IPCC Energy and Industry Subgroup, Response Strategies Working Group*, Paris, Cambridge University Press, Cambridge, UK.

Keppler, J., J. T. G. Hamilton, M. J. Bra, and T. Röckmann, 2006, Methane emissions from terrestrial plants under aerobic conditions, *Nature*, 439: 187–191.

Lean, J., and D. Rind, 1996, The Sun and climate, *Consequences,* 2(1), 27–36.

Lisiecki, L. E., and M. E. Raymo, 2005, A Pliocene-Pleistocene stack of 57 globally distributed benthic $\delta^{18}O$ records, *Paleoceanography,* 20, PA1003.

Madronich, S., 1993, Trends in surface radiation, *The Role of the Stratosphere in Global Change,* M. Chanin (ed.), Springer-Verlag, Berlin.

Molina, M. J., and F. S. Rowland, 1974, Stratospheric sink for chlorofluormethanes: Chlorine atom catalyzed destruction of ozone, *Nature,* 249, 810–812.

McGuffie, K., and A. Henderson-Sellers, 2005, *A Climate Modelling Primer,* 3rd ed, John Wiley & Sons, West Sussex, England.

Nakicenovic, N., 1996, Energy primer, in *Climate Change 1995: Impacts, Adaptations and Mitigation of Climate Change: Scentific-Technical Analyses, Intergovernmental Panel on Climate Change,* Cambridge University Press, Cambridge, UK.

National Research Council, Committee on Radiative Forcing Effects on Climate, 2005, *Radiative Forcing of Climate Change: Expanding the Concept and Addressing Uncertainties,* National Academy Press, Washington, DC.

National Research Council, Panel on Climate Change Feedbacks, 2003. *Understanding Climate Change Feedbacks,* National Academy Press, Washington, DC.

Pacala, S., and R. Socolow, 2004, Stabilization wedges: Solving the climate problem for the next 50 years with current technologies, *Science,* 305(5686), 968–972.

Petit, J. R., J. Jouzel, D. Raynaud, N. I. Barkov, J. M. Barnola, I. Basile, M. Bender, J. Chappellaz, J. Davis, G. Delaygue, M. Delmotte, V. M. Kotlyakov, M. Legrand, V. Lipenkov, C. Lorius, L. Pépin, C. Ritz, E. Saltzman, and M. Stievenard, 1999, Climate and atmospheric history of the past 420,000 years from the Vostok ice core, Antarctica, *Nature*, 399, 429–436.

Reddy, A. K. N., and J. Goldemberg, 1990, Energy for the developing world, *Scientific American*, September, 263(3), 110–118.

Simon, P. C., 1993, Atmospheric changes and UV-B monitoring, *The Role of the Stratosphere in Global Change*, M. Chanin (ed.), Springer-Verlag, Berlin.

Swisher, J. N., and G. M. Masters, 1991, Buying environmental insurance: Prospects for trading of global climate-protection services, *Climatic Change*, 19, 233–240.

Schneider, S. H., and J. Lane, 2006, *Avoiding Dangerous Climate Change*, H. J. Schellnhuber (ed.), Cambridge University Press, Cambridge.

Siegenthaler, U., T. F. Stocker, E. Monnin, D. Lüthi, J. Schwander, B. Stauffer, D. Raynaud, J. Barnola, H. Fischer, V. Masson-Delmotte, and J. Jouzel, 2005, Stable carbon cycle–climate relationship during the late Pleistocene, *Science*, 25, 310, 5752, 1313–1317.

Spahni, R., J. Chappellaz, T. K. Stocker, L. Loulergue, G. Hausammann, K. Kawamura, J. Flückiger, J. Schwander, D. Raynaud, V. Masson-Delmotte, and J. Jouzel, 2005, Atmospheric methane and nitrous oxide of the late Pleistocene from Antarctic ice cores, *Science*, 310(5752), 1317–1321.

United Nations Environment Programme (UNEP), 1994, *Montreal Protocol on Substances that Deplete the Ozone Layer, Scientific Assessment of Ozone Depletion*, World Meteorological Organization Global Ozone Research and Monitoring Project—Report No. 37, Geneva, Switzerland.

Warren, S. G., and S. H. Schneider, 1979, Seasonal simulation as a test for uncertainties in the parameterization of a Budkyo-Zellers zonal climate model, *Journal of the Atmospheric Sciences*, 36, 1377–1391.

Wuebbles, D. J., 1995, Weighing functions for ozone depletion and greenhouse gas effects on climate, *Annual Review of Energy and Environment*, 20, 45–70.

Wigley, T., and S. Raper, 2001, Interpretation of high projections for global-mean warming, *Science*, 293(5529), 451–454.

World Meteorological Organization (WMO), 2002, *The Scientific Assessment of Ozone Depletion, 2002*.

Worrell, E., L. Price, N. Martin, C. Hendriks, and L. Meida, 2001, Carbon dioxide emissions from the global cement industry, *Annual Review of Energy and the Environment*, 26, 303–329, November.